BRL

REPORT NO. 1168
JULY 1962



# AN EXPERIMENTAL INVESTIGATION OF POSSIBLE ALUMINUM ADDITIVE CONTRIBUTIONS TO UNSTABLE COMBUSTION IN SOLID ROCKET PROPELLANTS



Leland A. Watermeier
William P. Aungst
Samuel P. Pfaff

Department of the Army Project No. 517-06-002
Ordnance Management Structure Code No. 5010.11.585

BALLISTIC RESEARCH LABORATORIES

ABERDEEN PROVING GROUND, MARYLAND

B A L L I S T I C  R E S E A R C H  L A B O R A T O R I E S

REPORT NO. 1168

JULY 1962

# AN EXPERIMENTAL INVESTIGATION OF POSSIBLE ALUMINUM ADDITIVE CONTRIBUTIONS TO UNSTABLE COMBUSTION IN SOLID ROCKET PROPELLANTS

Leland A. Watermeier
William P. Aungst
Samuel P. Pfaff



Interior Ballistics Laboratory

Department of the Army Project No. 517-06-002
Ordnance Management Structure Code No. 5010.11.585

A B E R D E E N  P R O V I N G  G R O U N D,  M A R Y L A N D

B A L L I S T I C  R E S E A R C H  L A B O R A T O R I E S

REPORT NO. 1168

LAWatermeier/WPAungst
SPPfaff/bn
Aberdeen Proving Ground, Md.
July 1962

# AN EXPERIMENTAL INVESTIGATION OF POSSIBLE ALUMINUM ADDITIVE CONTRIBUTIONS TO UNSTABLE COMBUSTION IN SOLID ROCKET PROPELLANTS

## ABSTRACT

Composite - double base rocket propellant slabs which contained different concentrations and particle sizes of aluminum were burned in a transparent-walled chamber. The chamber was exhausted to the atmosphere. The slabs were ignited in cigarette fashion and burned under ambient nitrogen pressures of 200-800 psi. Experimental runs were made under steady flow conditions and under oscillating conditions with a siren rotating over the exhaust port.

Motion pictures were taken of the burning process at high framing rates. Data on droplet burning and concentrations in various regions above the propellant surfaces were obtained from individual frames of the film.

The rate of growth and rate of burning or evaporation of the aluminum droplets on the surface and in the flame zone are discussed. Agglomeration of aluminum on the propellant surface was appreciable and was a function of chamber pressure and initial aluminum concentration. As droplets of aluminum left the surface, they vibrated at

frequencies near those predicted by the Rayleigh assumption for liquid droplets.[11] Concentration measurements did not support the postulation that this process could be a factor in low frequency combustion instability, however.

A low frequency variation of the measured mass flux of aluminum above the propellant surface was found. It is concluded that this type of variation is probably a major contributor to low frequency phenomena reported in firings of some highly aluminized propellant systems. It also provides a partial explanation for low frequency luminosity variations reported by some investigators.

TABLE OF CONTENTS

LIST OF ILLUSTRATIONS

LIST OF ILLUSTRATIONS (Cont'd)

## INTRODUCTION

Interest in the combustion of metal powders has increased considerably over the last few years. Much of this interest has been motivated by the inclusion of metals, aluminum in particular, in solid propellant formulations[1]. These metals act as combustion instability suppressants and as sources of additional energy. For a few years powdered aluminum occupied the unique position of being probably the best cure for unstable combustion when added to solid rocket propellants. This position has recently been challenged and it is now feared that aluminum may actually contribute to or cause low frequency combustion instability, in some cases, rather than cure it. It seemed to us that observations of aluminum agglomeration on burning double base propellant surfaces by Angelus of ABL and on composite propellant surfaces made by our group at BRL[2] might be quite significant in this problem. Therefore a series of experiments were conducted in the Interior Ballistics Laboratory to further investigate the possible role of aluminum in low frequency instabilities. The approach used was to burn individual propellant slabs in a windowed chamber at high pressures and to photograph the combustion process. The propellants contained different percentages and different particle sizes of aluminum. The results of some of these experiments are given in this paper. Some of the data on droplet burning have been treated in the manner of liquid droplet evaporation which has been used in investigations of liquid propellant systems.

## 1. EXPERIMENTAL APPARATUS

The propellant slabs were burned in a windowed chamber (fig. 1). It was exhausted to the atmosphere either through a vent plate or through a slotted wheel (siren). The chamber is made of brass and is a parallelepiped measuring approximately 1-1/4 x 4-1/4 x 1-3/4 inches internally. The windows which form the sides of the chamber are made of 3/4 inch thick plastic. An elevator was used to maintain the propellant burning surface at a particular level in the chamber during a run.

Pressure gauges (Dynisco and Dynagauge) were located at the burning surface level and at the end of the test chamber. These pick-ups recorded chamber pressure variations at their respective locations during an experimental run. They were recorded on an oscillograph recorder and on magnetic tape.

Nitrogen was used to raise the chamber pressure to the desired operating level and was used as an inhibitor as it flowed past the non-burning sides of the propellant slab. A schematic of the nitrogen flow system is shown in figure 2. The flow was maintained by four pressurized tanks attached to a manifold. The manifold was connected to a pressure reducing valve and thence to a flow rate meter, a line with a critical orifice, and the elevator housing. A diffusion plate in the test chamber provided for laminar flow past the sides of the propellant sample.

High speed motion pictures (2000 to 4500 pictures per second) of the burning surfaces and flame zones of the slabs were taken through the test chamber windows. A Fairchild 16 mm Motion Analysis camera was used. Lens systems yielding magnifications up to 2.5:1 were used. This magnification was further enhanced for film reading purposes by using a Kodak Contour projector with ratios up to 100:1. Both color and black and white film were used. Neutral density filters were incorporated on occasions. Front and rear lighting was furnished when needed by pre-focused 300-watt flood lamps.

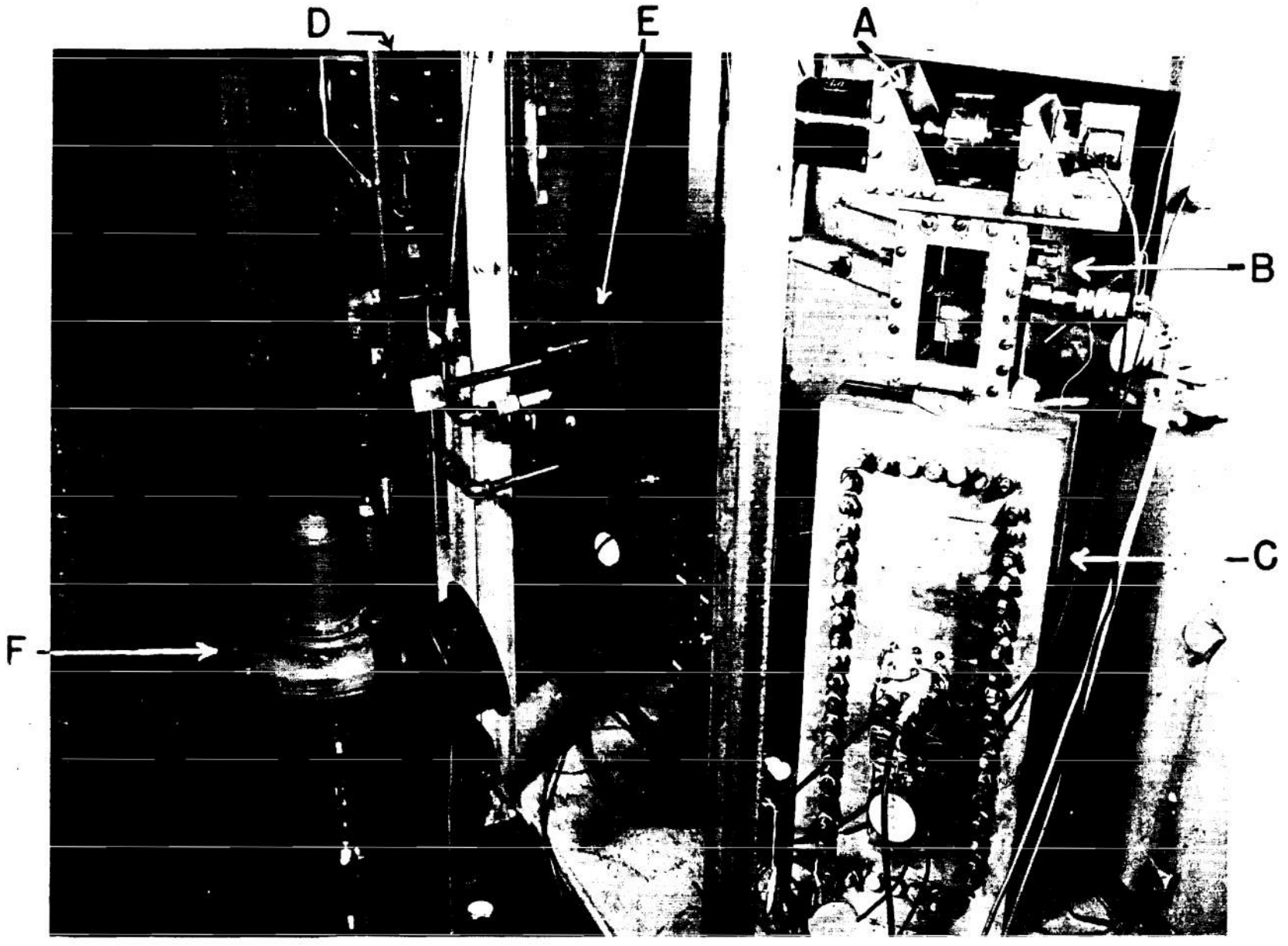


Figure 1. Photograph of experimental apparatus: A = siren assembly, B = test chamber, C = elevator housing, D = flowrator, E = regulator, F = Conoflow valve.

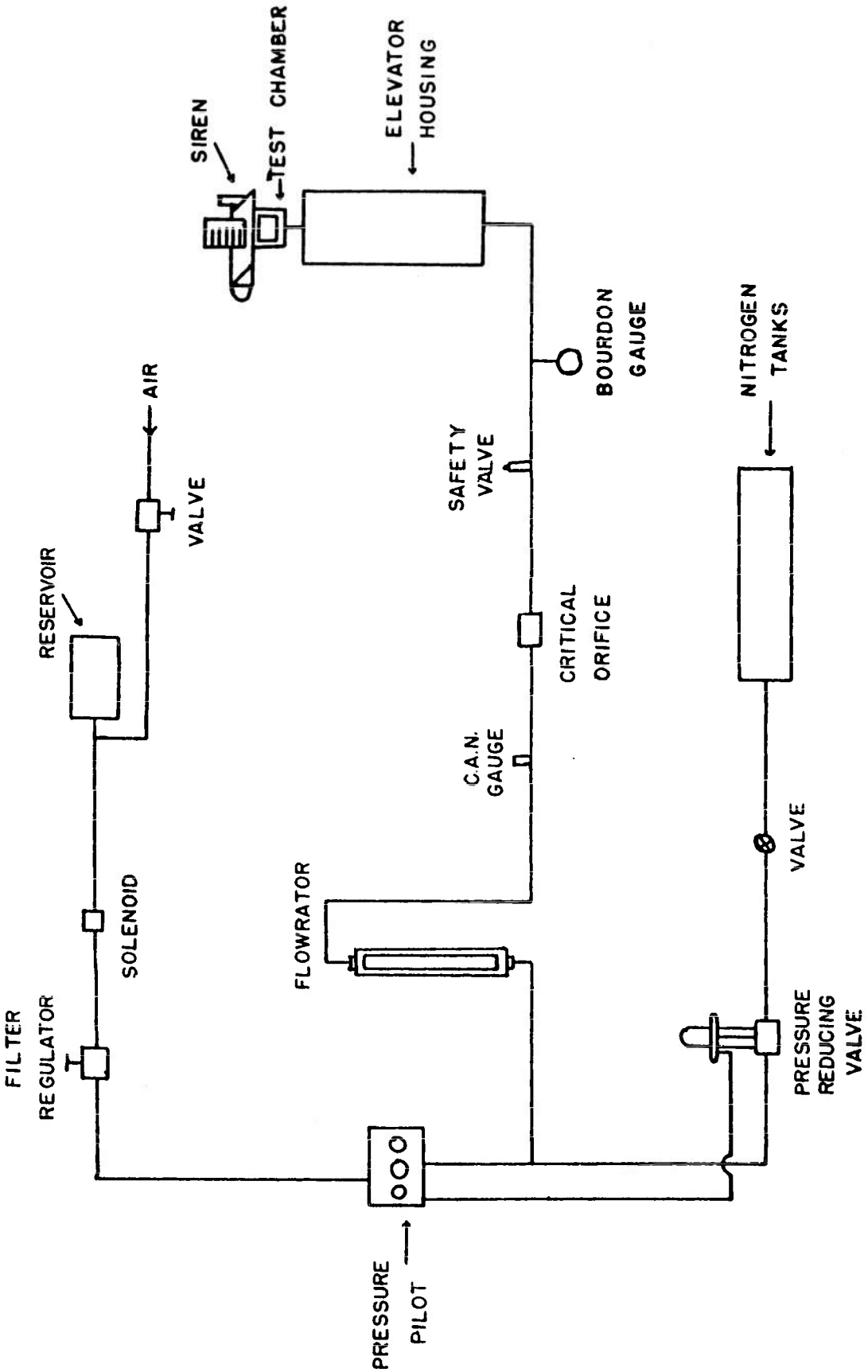


Figure 2. Schematic of nitrogen pressurizing system

## 2. EXPERIMENTAL APPROACH

### 2.1 Technique

The technique used in these experiments consisted of burning 1/4 x 3/4 x 1-1/4 inch slabs of propellant, cigarette fashion, in a limited pressure range simulating rocket chamber conditions. The pressure range investigated was 200 to 900 psi. The slabs were ignited on the 1/4 x 3/4 inch edge and were burned in an upright position in the test chamber. A hot wire - combustible paste ignition system was used. Inked lines were placed on the sides of the slab as standard distance references. Supplementary standards were provided by wires projecting from the chamber walls. The slabs were photographed during the burning process and measurements were made subsequently from the film. Fiducial timing dots were placed along the sides of the film by a generator. The dots provided millisecond time references. Pressure records were made during each run and time - pressure relationships were compared with phenomena observed on the motion picture film.

In some experimental runs, the siren was pulled over the vent hole approximately one or two seconds after ignition. Pressure waves or variations normal to the burning surface of the propellant were introduced in this manner. Observations could then be made on aluminum droplet behavior under steady and under oscillating conditions.

### 2.2 Propellants

The propellants chosen for this study were of the type using nitrocellulose - nitroglycerin - ammonium perchlorate - aluminum. The aluminum was procured from two different companies, namely, Alcoa and Reynolds. It was incorporated in the propellants in 2, 10, and 20 per cent by weight fractions. Three different ranges of particle sizes were used: 5-8 microns, 20 microns, and 43-143 microns. The lot numbers are shown in Table 1. In Table 2 are shown the computed

| Per cent by Weight of Al ↓ / Type and Diameter of Al → | REY 28 XD Flake ( 5 micron) | REY 400 (5 ± 2 micron) | REY 120 (20 ± 5 micron) | ALCOA 140 (6-8 micron) | ALCOA 101 (43-143 micron) |
|---|---|---|---|---|---|
| 2% | 220 | 217 | 211 | 226 | 223 |
| 10% | 221 | 218 | 212 | 227 | 224 |
| 20% | 222 | 219 | 229 | 228 | 225 |

Table 1. Lot Numbers of the Propellants Used in This Investigation.

| Composition (% by Wt.) | $P_c$ (PSI) | $T_c$ ($^\circ$K) | mols Products Per 100 gms | mole Wt. Prod. Gases | MAJOR PRODUCTS: mols CO | mols $CO_2$ | mols $H_2$ | mols HCl | mols $H_2O$ | mols $N_2$ | mols $Al_2O_3$ |
|---|---|---|---|---|---|---|---|---|---|---|---|
| 2Al<br>47.5 AP<br>10 NC<br>25 NG<br>Lots 211, 217, 220, 223, 226 | 1000 | 3135 | 3.732 | 26.79 | .7321 | .5417 | .2310 | .3739 | 1.278 | .4167 | .0368 |
| | 900 | 3128 | 3.735 | 26.77 | .7334 | .5405 | .2320 | .3730 | 1.276 | .4167 | .0368 |
| | 800 | 3120 | 3.738 | 26.75 | .7347 | .5392 | .2330 | .3721 | 1.273 | .4166 | .0368 |
| | 700 | 3110 | 3.741 | 26.73 | .7363 | .5376 | .2343 | .3710 | 1.271 | .4165 | .0368 |
| | 600 | 3098 | 3.745 | 26.70 | .7380 | .5358 | .2357 | .3698 | 1.268 | .4164 | .0368 |
| | 500 | 3085 | 3.750 | 26.67 | .7403 | .5336 | .2375 | .3683 | 1.264 | .4163 | .0368 |
| | 400 | 3068 | 3.756 | 26.62 | .7429 | .5310 | .2396 | .3664 | 1.260 | .4162 | .0368 |
| | 300 | 3045 | 3.764 | 26.57 | .7464 | .5275 | .2425 | .3639 | 1.254 | .4161 | .0368 |
| | 200 | 3012 | 3.775 | 26.49 | .7513 | .5226 | .2467 | .3602 | 1.245 | .4159 | .0368 |
| | 100 | 2954 | 3.795 | 26.35 | .7593 | .5146 | .2542 | .3538 | 1.230 | .4157 | .0368 |
| 10 Al<br>39.5 AP<br>10 NC<br>25 NG<br>Lots 212, 218, 221, 224, 227 | 1000 | 3397 | 3.551 | 28.16 | 1.042 | .2320 | .5019 | .3024 | .8803 | .3834 | .1836 |
| | 900 | 3388 | 3.555 | 28.13 | 1.042 | .2316 | .5025 | .3015 | .8780 | .3833 | .1836 |
| | 800 | 3378 | 3.558 | 28.11 | 1.043 | .2312 | .5031 | .3005 | .8753 | .3833 | .1836 |
| | 700 | 3366 | 3.563 | 28.07 | 1.043 | .2306 | .5038 | .2993 | .8723 | .3832 | .1835 |
| | 600 | 3352 | 3.568 | 28.03 | 1.044 | .2300 | .5047 | .2980 | .8687 | .3831 | .1835 |
| | 500 | 3336 | 3.574 | 27.98 | 1.045 | .2293 | .5057 | .2964 | .8645 | .3830 | .1834 |
| | 400 | 3315 | 3.581 | 27.93 | 1.045 | .2284 | .5069 | .2943 | .8592 | .3830 | .1834 |
| | 300 | 3288 | 3.591 | 27.84 | 1.047 | .2273 | .5084 | .2917 | .8523 | .3828 | .1833 |
| | 200 | 3248 | 3.606 | 27.73 | 1.048 | .2258 | .5106 | .2878 | .8424 | .3827 | .1832 |
| | 100 | 3178 | 3.631 | 27.54 | 1.050 | .2236 | .5141 | .2812 | .8258 | .3825 | .1830 |
| 20 Al<br>29.5 AP<br>10 NC<br>25 NG<br>Lots 219, 222, 225, 228, 229 | 1000 | 3657 | 3.345 | 29.89 | 1.226 | .0437 | .9442 | .1924 | .2926 | .3423 | .3402 |
| | 900 | 3646 | 3.350 | 29.85 | 1.226 | .0465 | .9419 | .1915 | .2922 | .3423 | .3395 |
| | 800 | 3633 | 3.354 | 29.81 | 1.226 | .0466 | .9396 | .1906 | .2917 | .3424 | .3389 |
| | 700 | 3617 | 3.360 | 29.76 | 1.226 | .0467 | .9370 | .1896 | .2910 | .3424 | .3382 |
| | 600 | 3599 | 3.366 | 29.71 | 1.226 | .0469 | .9340 | .1885 | .2902 | .3425 | .3374 |
| | 500 | 3578 | 3.374 | 29.64 | 1.226 | .0470 | .9302 | .1872 | .2893 | .3425 | .3365 |
| | 400 | 3552 | 3.384 | 29.55 | 1.226 | .0472 | .9256 | .1855 | .2880 | .3425 | .3354 |
| | 300 | 3518 | 3.396 | 29.44 | 1.226 | .0475 | .9195 | .1834 | .2861 | .3425 | .3342 |
| | 200 | 3469 | 3.414 | 29.29 | 1.226 | .0478 | .9110 | .1806 | .2832 | .3425 | .3326 |
| | 100 | 3386 | 3.446 | 29.02 | 1.225 | .0483 | .8957 | .1755 | .2775 | .3425 | .3301 |

Table 2. Composition of Propellant Samples Used Together with Computed Flame Temperatures and Major Product Concentrations Over The Pressure Range Studied.

flame temperatures and major equilibrium products obtained in the pressure ranges observed. These values were calculated using the method of Baer, Geene, et al.[3] The flame temperatures are shown to be essentially constant over the pressure range studied for each of the three percentages.

## 3. EXPERIMENTAL RESULTS AND ANALYSIS

Approximately two-hundred and fifty experimental firings were made. The data obtained gave information on both surface and flame zone events.

### 3.1 Surface Phenomena, Melting and Agglomeration

The aluminum appeared to melt on the propellant surface in all the cases observed. In many instances it started to burn or vaporize there. This was in evidence as smoke, vapor, or flame trails projecting from the droplet on the surface upward into the flame zone (fig. 3). In frame to frame observations from the motion pictures, tiny droplets of aluminum could be seen forming on the propellant burning surface as a result of melting. The droplets usually did one of two things: (a) they grew in diameter as they rolled around on the surface, picked up or coalesced with other droplets and then rose into the flame zone or (b) they remained fixed in place for a few milliseconds, grew only a slight bit in diameter, and then were released into the flame zone. The rolling motion and diameter growth on the surface is thought to be strong evidence of surface agglomeration. In some instances, especially at high pressures and with high initial aluminum concentration, the propellant burning surface would appear to be almost covered with a blanket of molten aluminum. As many of the droplets were ready to leave the surface, they would cling momentarily by a cord or thread of molten metal and then be released (fig. 3).

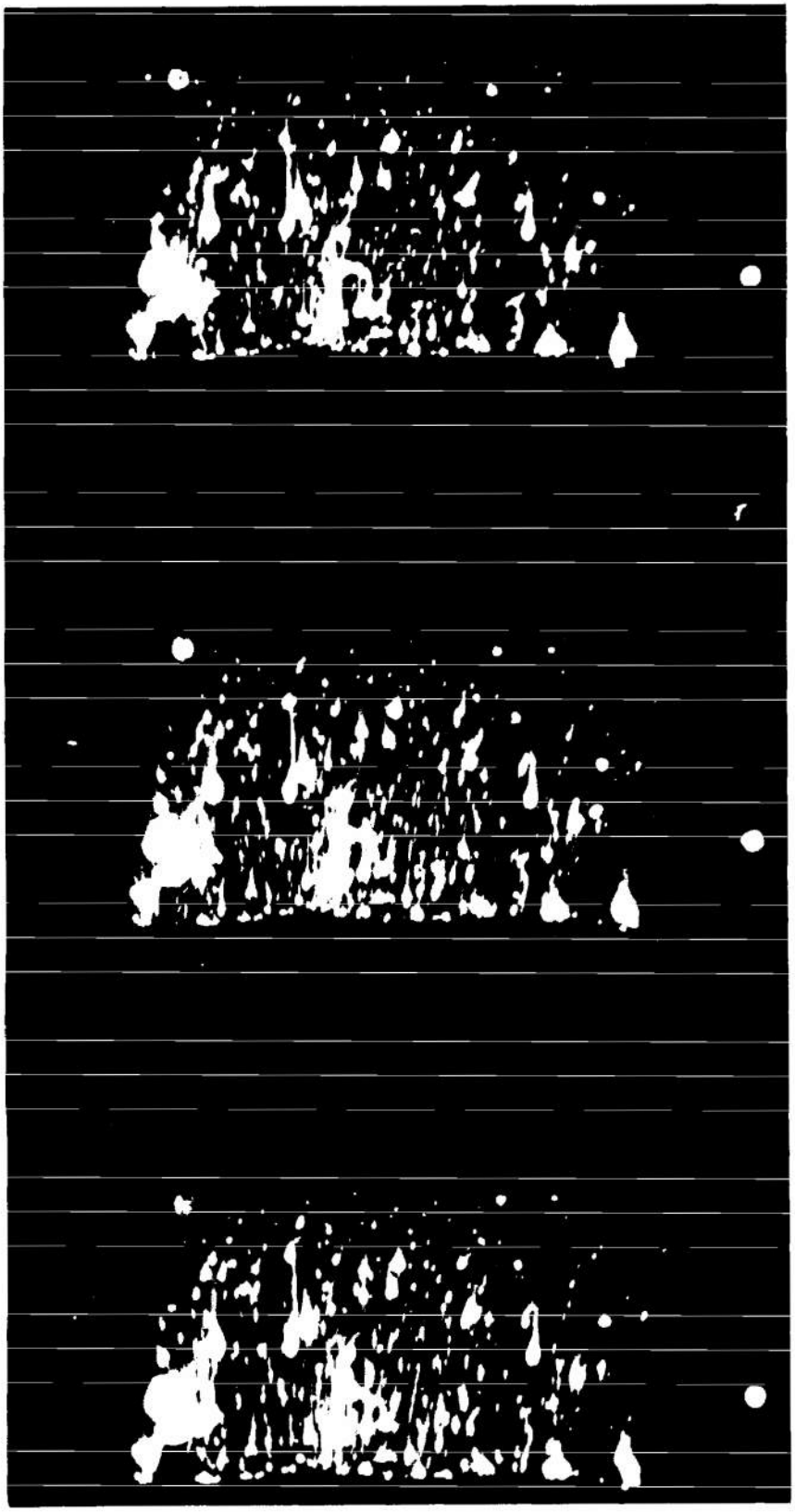

Figure 3. Consecutive frames (3800/sec) from film of propellant lot 225 burning at 200 psi. Note vapor trails from the droplets and surface formation of agglomerates.

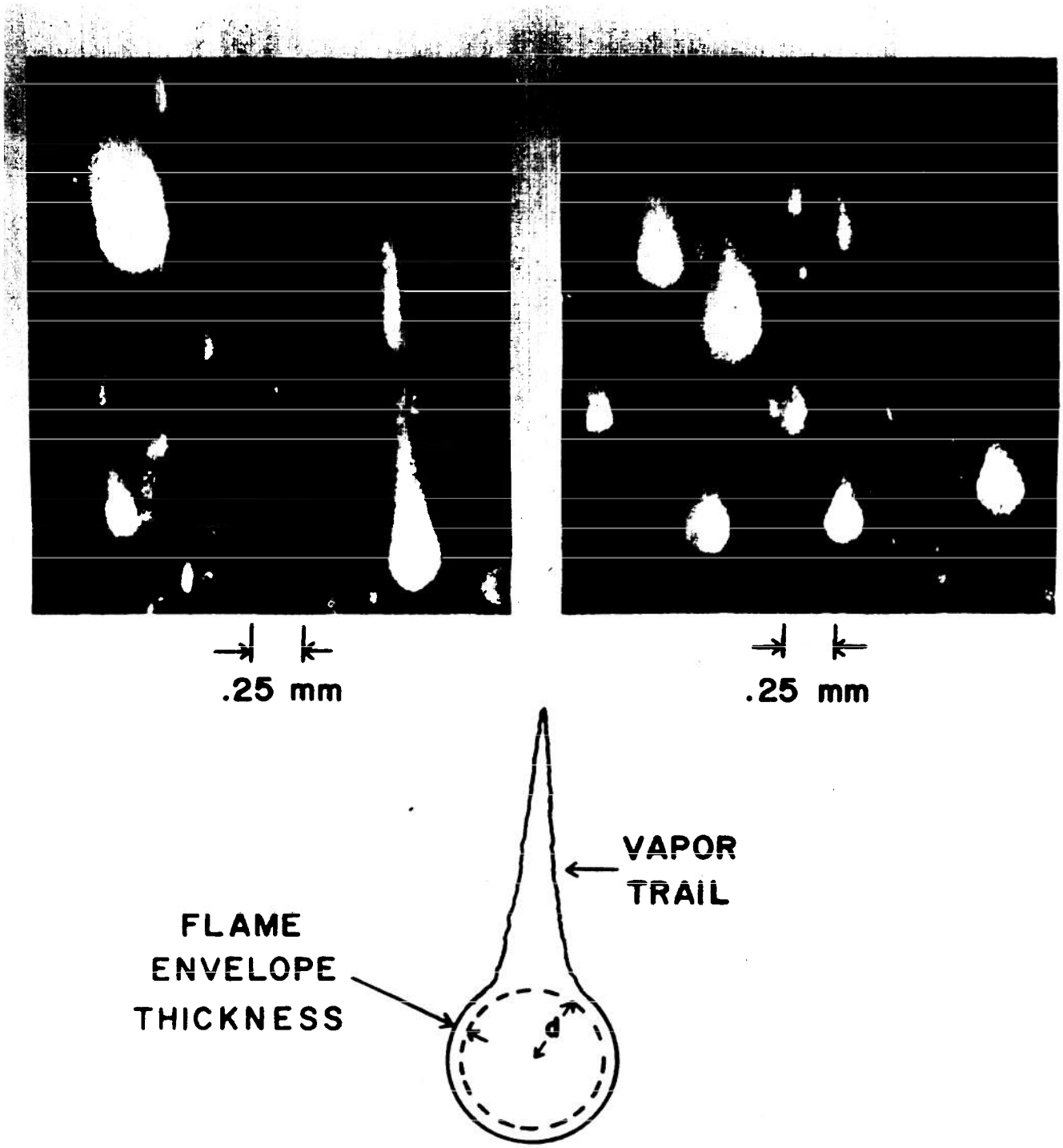


Figure 4. Enlargements of burning droplets showing the vapor trails. The schematic drawing illustrates the flame envelope surrounding the liquid droplet. The envelope thickness varied from approximately .02d at 800 psi to 15d at 200 psi as determined by silhouette lighting.

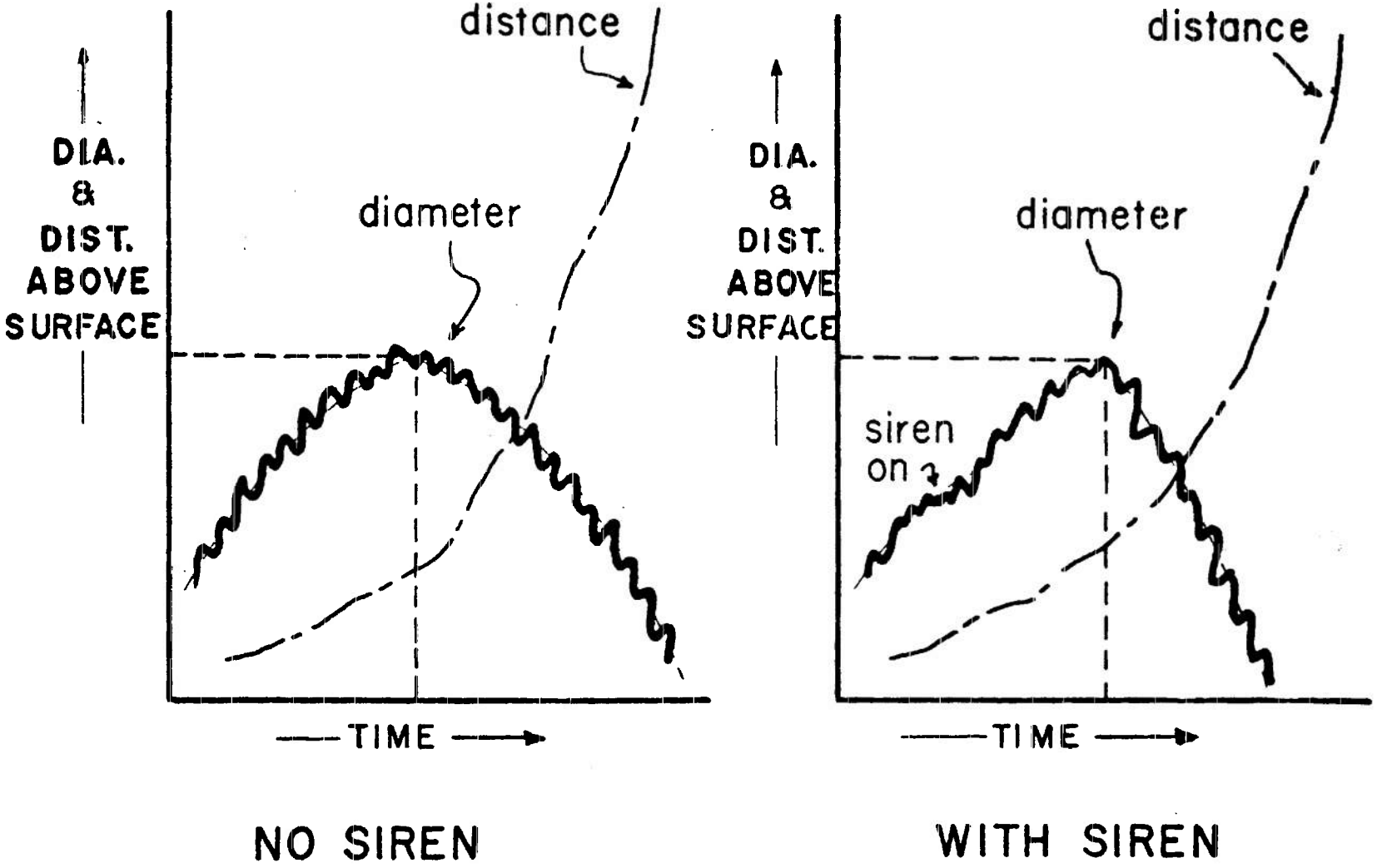


Figure 5. Typical plots of droplet diameter and distance above the propellant surface as functions of time.

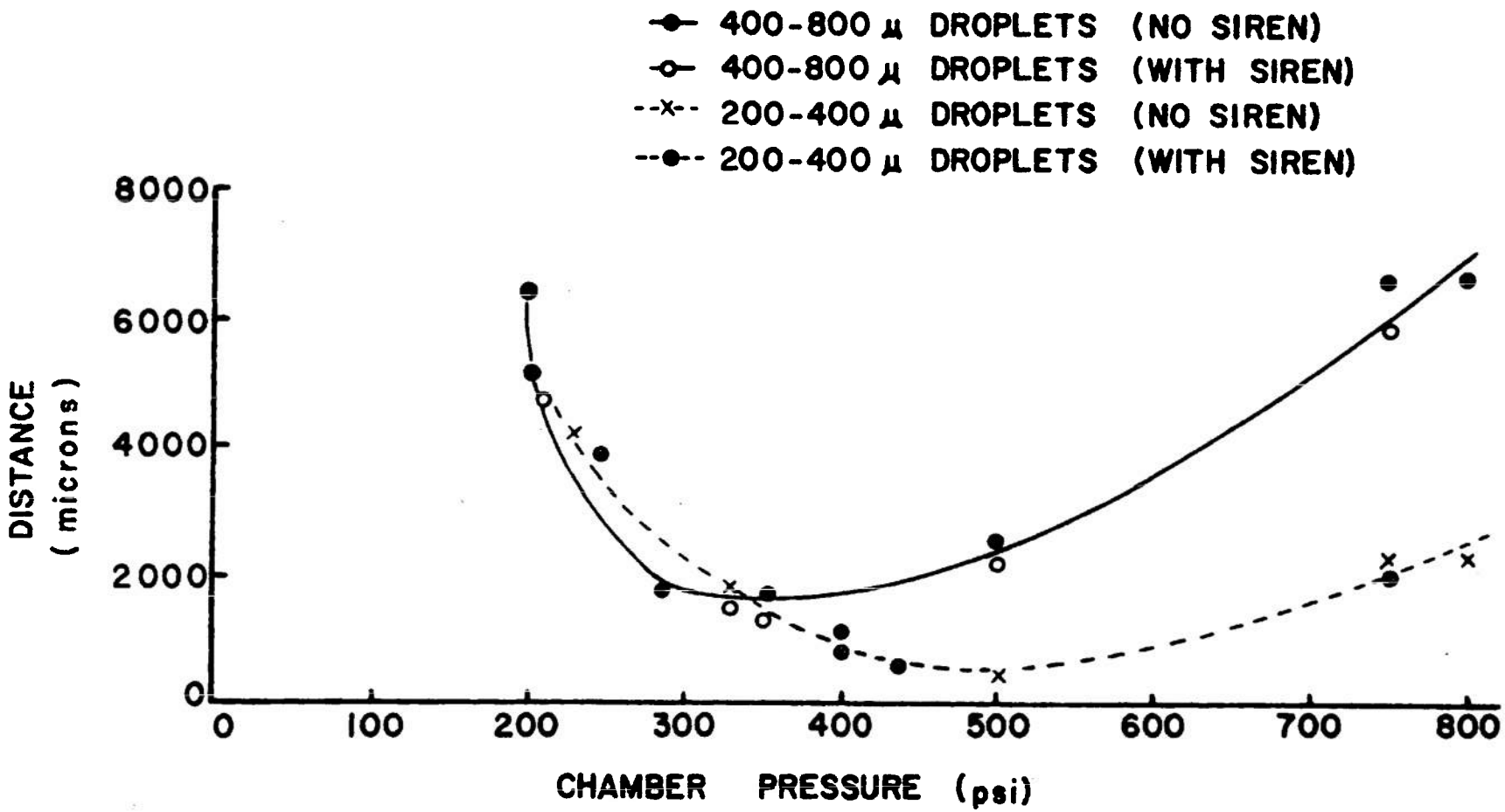


Figure 6. Plot of chamber pressure vs. distance above the burning propellant surface at which the droplets started decreasing in diameter. Siren pulsation had little or no influence on these distances.

## 3.2 Droplet Phenomena Above the Surface

As the droplets left the propellant burning surface, they assumed a semi-spherical shape, in most instances, with a vapor trail preceding them (fig. 4). They grew in diameter until they reached a certain level above the burning surface. At this level they would start to decrease in diameter (fig. 5). The rates of decrease of droplet diameters were increased under the influence of siren pulsing at 1100-1300 cps. The level above the surface at which the diameters started to decrease was not appreciably affected by the siren pulsing.

The propellant burning surface was assumed to be near a velocity antinode[2] in the chamber as the siren-driven oscillations were introduced. The pressure gauges located in the walls at this level verified the assumption to some extent. It is questionable, however, whether this condition actually exists near the burning surface since the surface itself may act as a local end plate.

It is postulated that the droplet growth phenomena above the surface could be, among other things, a result of (a) meteoric pelting of large liquid droplets by small particles which are beyond the resolution of the optical system, (b) ignition above the surface with an apparent diameter growth due to the formation of a flame envelope, or (c) hollow spheres or droplets which are inflating like balloons as the vapor pressure inside increases with temperature. The experimental evidence seems to lend more support to (a) or (b) as will be discussed in succeeding sections.

The distance above the surface at which the droplets started to evaporate or decrease rapidly are plotted vs. chamber pressure in figure 6. The particle diameters shown were arbitrarily divided into two ranges, i.e. 200-400 microns and 400-800 microns. The plot exhibits a profile which is expected until it reaches the higher pressures. There are at least two possible ways of explaining this discrepancy. In one case, the hot flame zone would be expected to

recede from the surface at low pressures and come closer to it at high pressures. At low pressures the droplets move far from the surface before appreciable evaporation takes place. At intermediate pressures, the droplets start evaporating closer to the surface. At the higher pressures, combined effects of increased mass flow rate of the product gases and an oxide insulation or protective layer on the droplets are evident as the droplets are carried further from the surface before starting to decrease in size. One thing must be kept in mind. The growth mechanism is probably present the entire time during which our data is taken so the point at which the diameter starts decreasing takes on more significance. It means that the evaporation or burning rate has overcome this gain mechanism and has, indeed, exceeded it by a significant amount. Some typical growth and decay rate data are shown in Table 3. Calculations were made on droplet histories assuming that they were pure aluminum. This, of course, would be complicated by any oxide formation. The droplets were treated as burning fuel in a flowing medium. The procedure and some of the aluminum properties used are contained in Appendices I and II. A typical plot of the rate of droplet decay as compared with two of the theoretical curves is shown in figure 7. Some of the computed evaporation times and distances above the surface for complete evaporation are shown in Table 4. On the basis of the computed histories and measured values, it appears that the data in Table 3 were obtained in temperature regions approximating 0.7 to 0.9 of the theoretical flame temperatures.

Another possible explanation for the distance vs. chamber pressure plot data would be based on the assumption that the reaction zone was extremely thin in all cases and that there is essentially a constant temperature throughout the measurable field. This assumption is not too bad considering the previous discussion. Then a strong controlling factor on the evaporation rate would be the concentration of the aluminum vapor. In other words, near the surface where there would be a large vapor concentration at some pressures the evaporation rate

| Chamber Pressure (psi) | DROPLET GROWTH: Diameter Expansion (cm) | DROPLET GROWTH: Time for Expansion (sec x $10^3$) | DROPLET GROWTH: Surface Area Growth Rate ($cm^2$/sec) | DROPLET DECAY: Diameter Decrease (cm) | DROPLET DECAY: Time for Decrease (sec x $10^3$) | DROPLET DECAY: Surface Area Decrease Rate ($cm^2$/sec) | Distance above Propellant Surface when Decrease Started (cm) |
|---|---|---|---|---|---|---|---|
| 200 | .510 → .0670 | 21.5 | .276 | .0670 → .0560 | 27.9 | .152 | .58 |
| 225 | .0400 → .0475 | 28.0 | .074 | .0475 → .0380 | 29.5 | .087 | .42 |
| 300 | .0238 → .0283 | 5.2 | .142 | .0283 → .0169 | 2.24 | .723 | .22 |
| 325 (w/siren) | .0400 → .0595 | 6.08 | 1.003 | .0595 → .0145 | 4.32 | 2.421 | .16 |
| 400 | .0285 → .0351 | 8.30 | .159 | .0351 → .0235 | 4.96 | .431 | .10 |
| 400 (w/siren) | .0240 → .0333 | 13.84 | .121 | .0333 → .0167 | 3.05 | .562 | .11 |
| 500 | .0350 → .0545 | 14.93 | .367 | .0545 → .0273 | 5.35 | .872 | .08 |
| 500 (w/siren) | .0273 → .0633 | 24.44 | .419 | .0633 → .0100 | 7.52 | 1.632 | .06 |
| 750 | .0272 → .0363 | 13.50 | .135 | .0363 → .0195 | 13.50 | .218 | .23 |
| 750 | .0575 → .0675 | 28.85 | .136 | .0675 → .0625 | 4.70 | .435 | .66 |



Table 3. Typical experimental growth and decay rates of droplets at various chamber pressures.

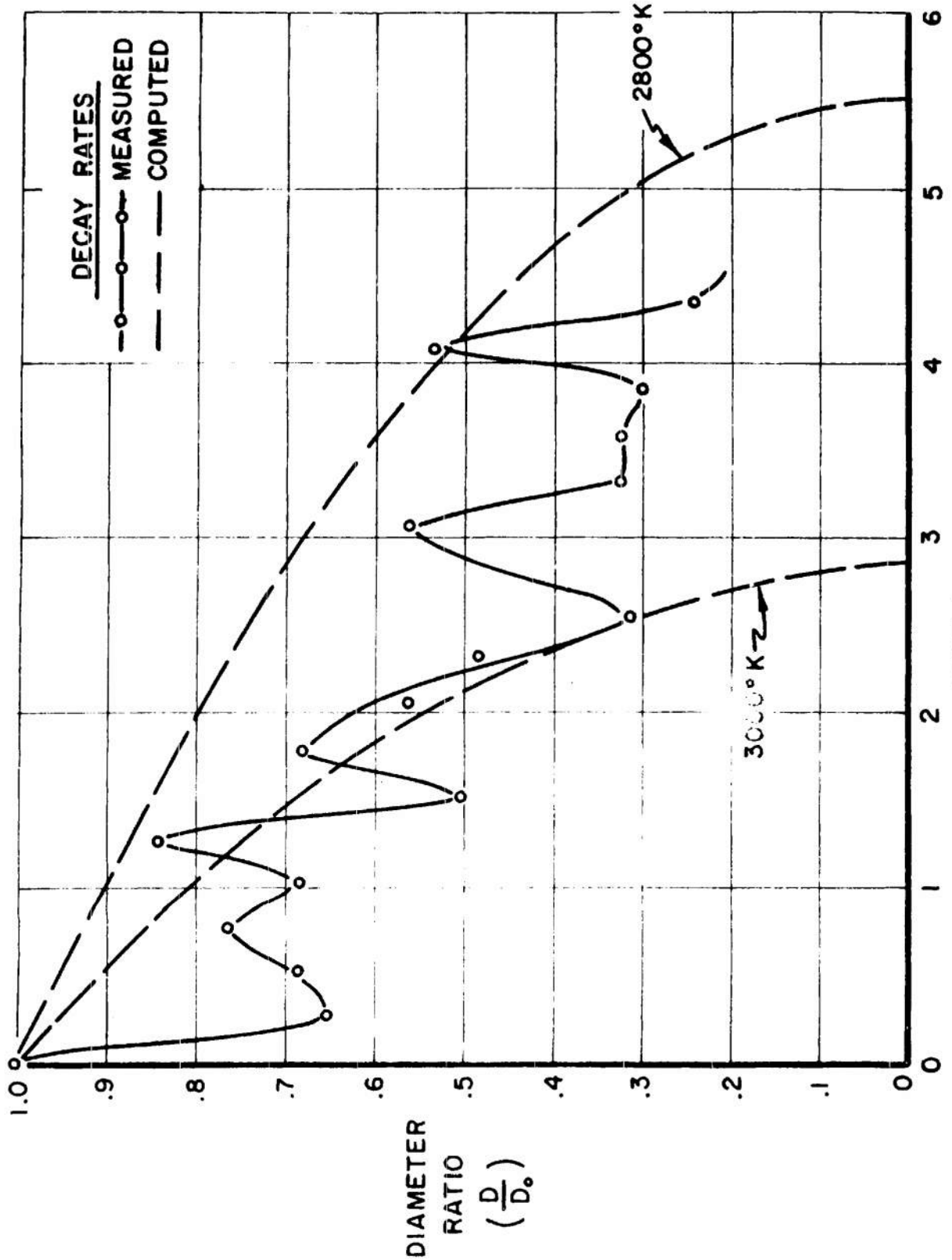


Figure 7. Plot of diameter ratio $(\frac{D}{D_o})$ as a function of time. Measured values and values computed by the procedure in Appendix I are compared for a droplet with $D_o$ = 600 microns. Propellant = Lot 228, Chamber Pressure = 300 psi

| $D_o$ (microns) | $T_f$ = 2600° K | | $T_f$ = 2800° K | | $T_f$ = 3000° K | |
|---|---|---|---|---|---|---|
| | Time to completely evap. (milliseconds) | Dist. above surface where $D_o \rightarrow 0$ (microns) | Time to completely evap. (milliseconds) | Dist. above surface where $D_o \rightarrow 0$ (microns) | Time to completely evap. (milliseconds) | Dist. above surface where $D_o \rightarrow 0$ (microns) |
| 50 | .897 | 363 | .462 | 186 | .238 | 96 |
| 100 | 1.794 | 728 | .924 | 373 | .476 | 191 |
| 200 | 3.584 | 1455 | 1.848 | 745 | .952 | 382 |
| 400 | 7.172 | 2912 | 3.696 | 1491 | 1.905 | 764 |
| 600 | 10.759 | 4369 | 5.544 | 2237 | 2.857 | 1145 |
| 800 | 14.347 | 5825 | 7.393 | 2982 | 3.810 | 1528 |
| 1000 | 17.930 | 7281 | 9.240 | 3728 | 4.762 | 1909 |

Table 4. Theoretical times for complete evaporation of aluminum droplets with various diameters as functions of three different flame temperatures, $T_f$. Distance above the propellant surface for complete droplet evaporation is also given.

would be low and the droplet would travel further from the surface before decreasing appreciably in size. This mechanism, then, would hinge more on vapor concentration and less on temperature considerations. This type of phenomenon has been discussed by Burgoyne and Cohen[4] on effects of drop size on flame propagation in liquid aerosols. They maintain that the mechanism of flame propagation is completely transformed within the droplet diameter range of 7 to 55 microns. Below 10 microns, the suspension behaves as a vapor and above 40 microns, the drops burn individually with one drop igniting adjacent ones. This process, they claim, leads to increased burning rates for the larger drops. Figure 8 shows consecutive frames from film of burning propellants containing 2 per cent and 20 per cent of aluminum, lots 217 and 219, respectively. The flame zone, in comparison, appears to be transformed from one of a diffusion or vapor flame in the 2 per cent composition to a zone of droplet burning in the 20 per cent composition. Therefore, the aluminum vapor theory may be quite applicable.

### 3.3 Droplet Vibrations

In all experimental runs in which the burning aluminum droplet histories could be traced, oscillations of the major and minor dimensions of the ellipsoidal droplets were observed. Measurements of frequency and amplitude were made. The vibration frequencies ranged from 500 to 1100 cps for droplets with mean diameters (average of major and minor dimensions) of 200 to 700 microns. The magnitude of the diameter variations was often quite large, i.e. 50 to 100 per cent. Vibrations of smaller droplets were discernible but the frequencies approached the photographic framing limits so these data were not analyzed. The frequency of vibration and amplitude of the oscillations were dependent upon particle diameter and chamber pressure.

When siren pulsations were introduced, the larger droplets ($>$200 microns) would assume a vibration frequency close to the siren

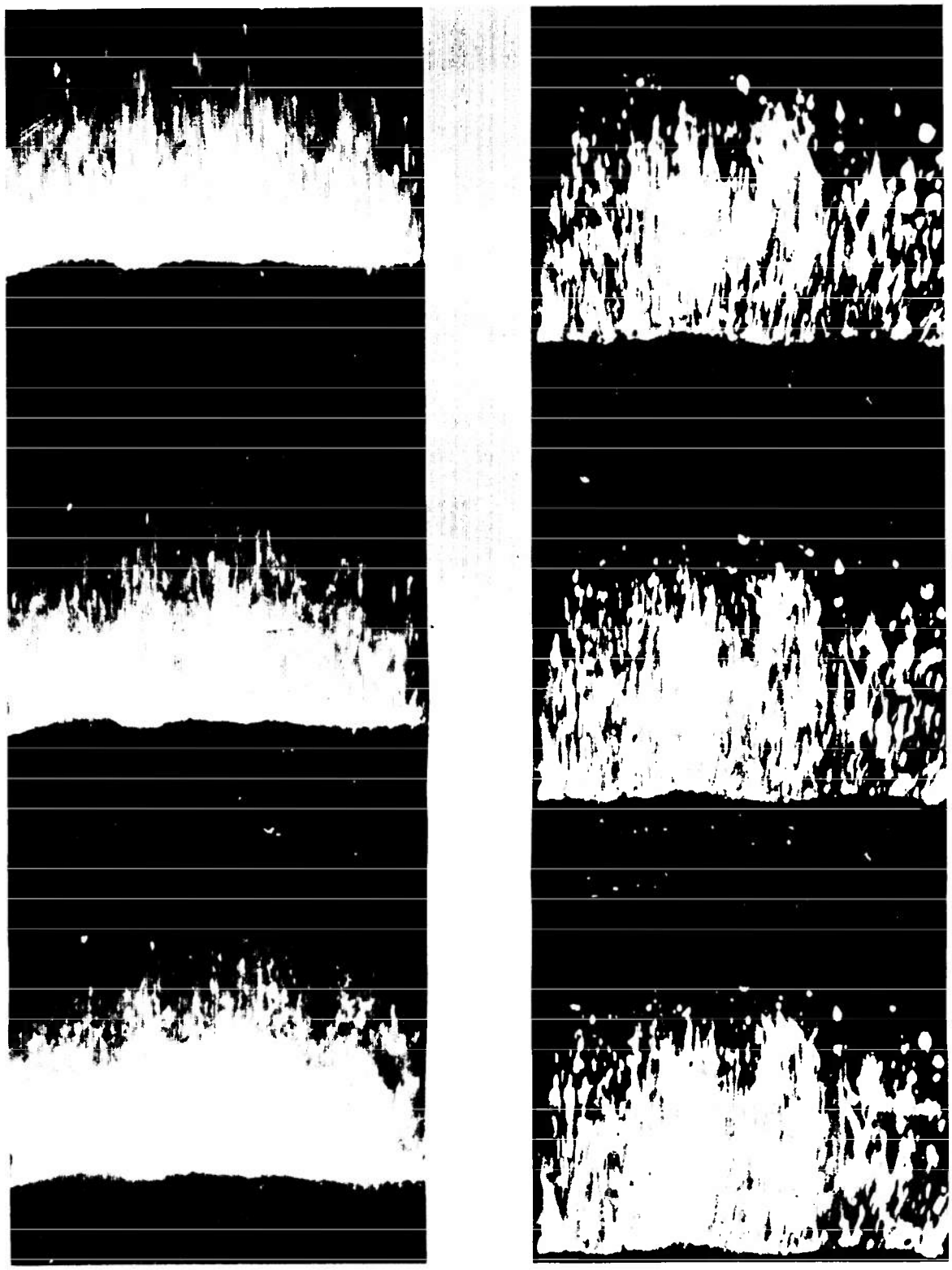

Figure 8. Enlargements of consecutive frames from film of burning propellant. On the left, lot 217 burning at chamber pressure of 390 psi. The framing rate was 2800 fps. On the right, lot 219 burning at chamber pressure of 405 psi. The framing rate was 3000 fps.

frequency. Their evaporation or burning rate would also be increased as was already discussed.

Two approaches were used to compute the natural vibration frequencies of the droplets in an undisturbed medium, i.e. no siren pulses introduced. In the first case, it was assumed that (a) the aluminum was molten on the burning propellant surface, and (b) it left the surface as liquid droplets which were set into vibration by the release from the surface. This vibratory motion did not damp out but continued with the surface tension of the liquid acting as a restoring force. Using Rayleigh's analysis[5] for the period of oscillation of droplets, the following relationship was obtained

$$\tau = \left(\frac{3\pi m}{8\sigma}\right)^{\frac{1}{2}} = 0.785 \left(\frac{\rho}{\sigma}\right)^{\frac{1}{2}} (d)^{\frac{3}{2}}$$

where $\tau$ = period of vibration, m = mass of the droplet, $\sigma$ = surface tension of the liquid, $\rho$ = liquid density and d = diameter of the droplet. Values of 2.2 grams/cm$^3$ and 250 dynes/cm were assumed for $\rho$ and $\sigma$, respectively, in all cases. These approximate values were assumed for a temperature near the boiling point of aluminum (2823$^\circ$K). The vibration frequencies of droplets ranging from 50 to 1000 microns in diameter were computed. These frequencies varied from 39000 to 400 cps, respectively.

In the second approach to theoretical vibration frequencies, it was assumed that (a) the aluminum melted on the surface and formed vapor filled bubbles which were ejected into the flame zone, and (b) the bubbles oscillated with a periodicity controlled by the properties of the wall and the enclosed vapor. Therefore, vibration frequencies of hollow, flexible spheres were computed according to the method of Morse and Feshbach[6]. Although the major and minor dimension variations we measured did not indicate symmetric vibrations, we assumed that this would provide a close enough approximation to the actual case. So their equations for symmetric vibrations were used as

$$\omega_{os} = \pi\gamma_{os}\, c/a$$

If the membrane is the restoring factor and controls the motion, they show that the lowest natural frequency will be

$$\pi\gamma_{01} \simeq \left(\frac{3\rho a}{\rho_s h}\right)^{\frac{1}{2}} \left[1 + \left(\frac{2Eh}{3\rho c^2 a}\right)\right]$$

where $\rho$ = density of gas inside sphere, a = equilibrium sphere radius, $\rho_s$ = wall density, h = wall thickness, c = sound velocity, and E = modulus of elasticity. Frequencies of the order of 30000 to 120000 cps were obtained for droplets whose diameters ranged from 1000 to 50 microns, respectively. Wall thicknesses were varied from less than 5 per cent to about 99 per cent of the droplet radius.

The theoretical vibration frequencies were several orders higher than those measured experimentally. We assumed therefore that the droplets under observation were not hollow. A comparison of some of the experimental values obtained and the frequencies computed from these two methods are shown in figure 9. Adjustments in the surface tension of the droplets could alter the relationships shown, of course.

Evidence of some hollow particles was found collected on cooler portions of the chamber, however. Photomicrographs of some of the residue is shown in figure 10. It is thought that if the amount of hollow droplets formed is significant, this process must occur at a distance further from the surface than we can observe in our film, namely, 1.6 cm.

## 3.4 Drag Forces on Droplets

The drag forces on some of the droplets in the non-pulsed runs were computed using the following equation

$$F = C_d\, \pi\, D^2\, \rho\, (U - V)^2/8$$

where F = drag force (dynes), $C_d$ = drag coefficient, D = droplet diameter,

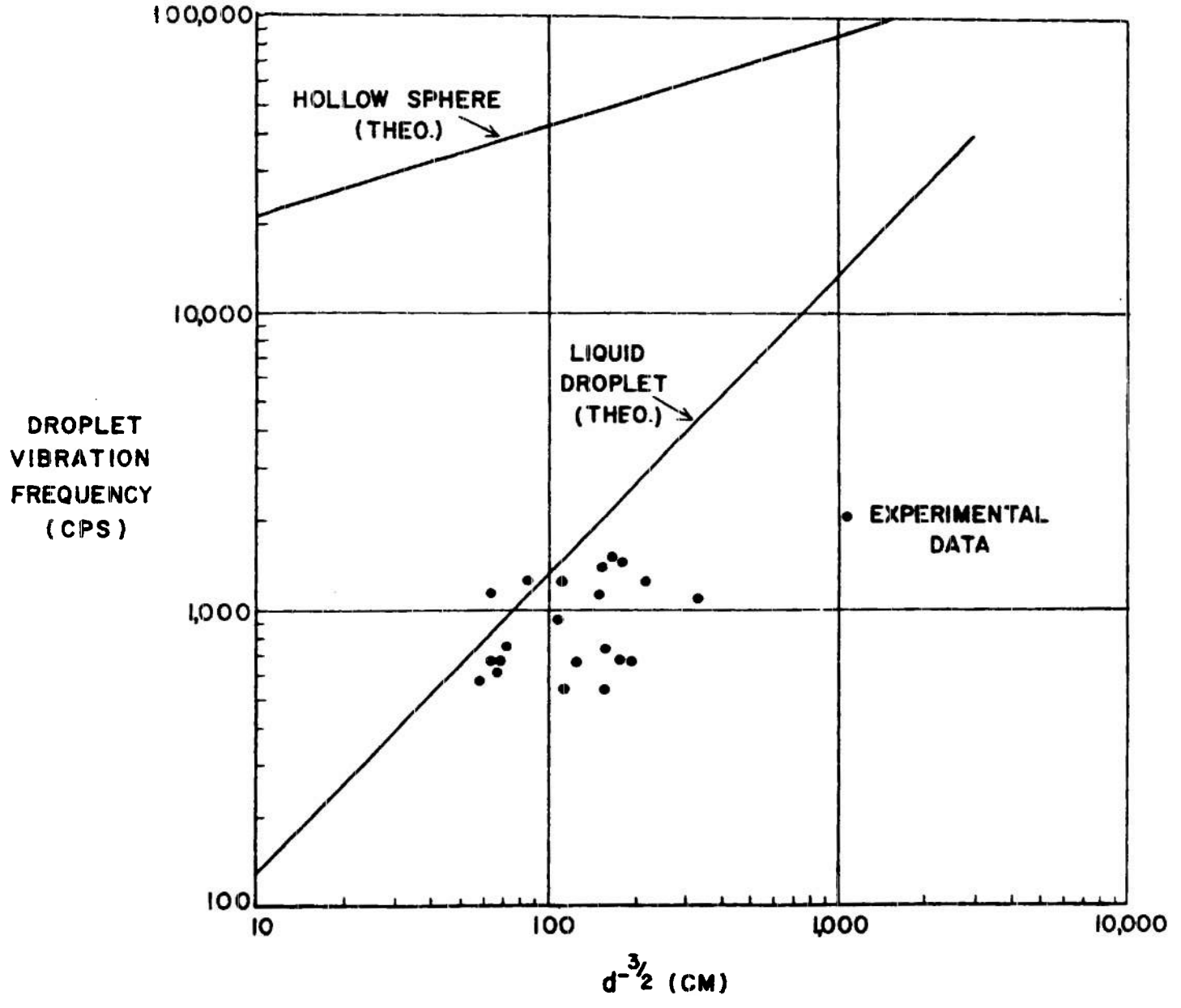


Figure 9. Plot of droplet vibration frequencies vs. $(\text{diameter})^{-3/2}$. The straight lines indicate theoretical values based on either hollow sphere or liquid droplet assumptions at the boiling point temperature of pure aluminum.

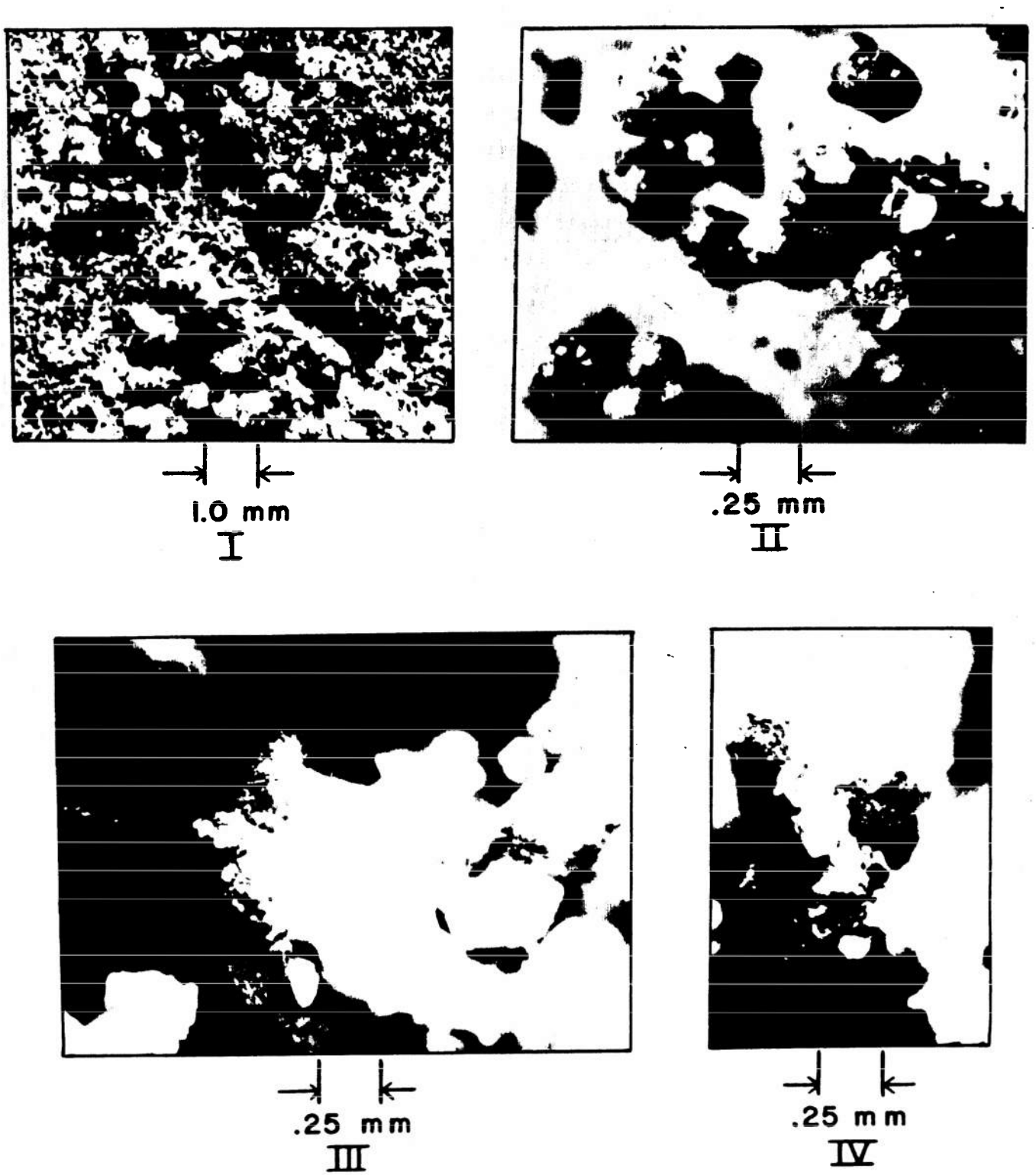


Figure 10. Photomicrographs of solidified residue collected in the test chamber from the burning aluminized propellants. Photo I shows many particles with holes in them. Photos II and III are enlargements of individual particles. Photo IV shows a particle that has apparently deflated after expelling enclosed gas.

$\rho$ = propellant gas density, U = propellant gas velocity, and V = droplet velocity. The D and V values were measured and $\rho$ and U values were computed. The $C_d$ values were obtained from Dodge and Thompson[7] which gives drag coefficients of a sphere as a function of the Reynolds number. In these experiments, the Reynolds number usually exceeded 0.4 so $C_d$ values were obtained from their graph.

Figures 11 through 15 show plots of some of the raw data obtained on droplet diameters and distances about the surface as a function of time. The computed drag forces for these particular cases are also plotted on the same time scale. It is noted that the drag force at any time, t, is reflected in a diameter variation and particle position variation above the surface. It would seem that this would be expected from the nature of the computations. However, it should be pointed out that two independent experimental measurements are involved here and they would not always bear the right relationship for the drag force exhibited unless the phenomena they represent were real. The drag forces on the droplets seem to depend largely upon the cross-sectional areas or diameters of the droplets that present resistance to the main stream flow.

## 3.5 Zone Concentrations and Aluminum Mass Flux

Measurements were made of size and distribution of visible droplets in various zones above the propellant surfaces. All data reported in this section were taken from runs in which siren pulses were not introduced. The data were obtained by placing the film in the Kodak projector and marking off zones of $\sim$ 200 micron thicknesses vertically above the surface. Then measurements were made in each zone over a series of frames. An approximate volume basis was established using the propellant thickness as the third dimension. Corrections were made for such things as (a) deviation from a vertical plane, (b) obscuring of smaller particles by larger ones and (c) depth of field or focus effects.

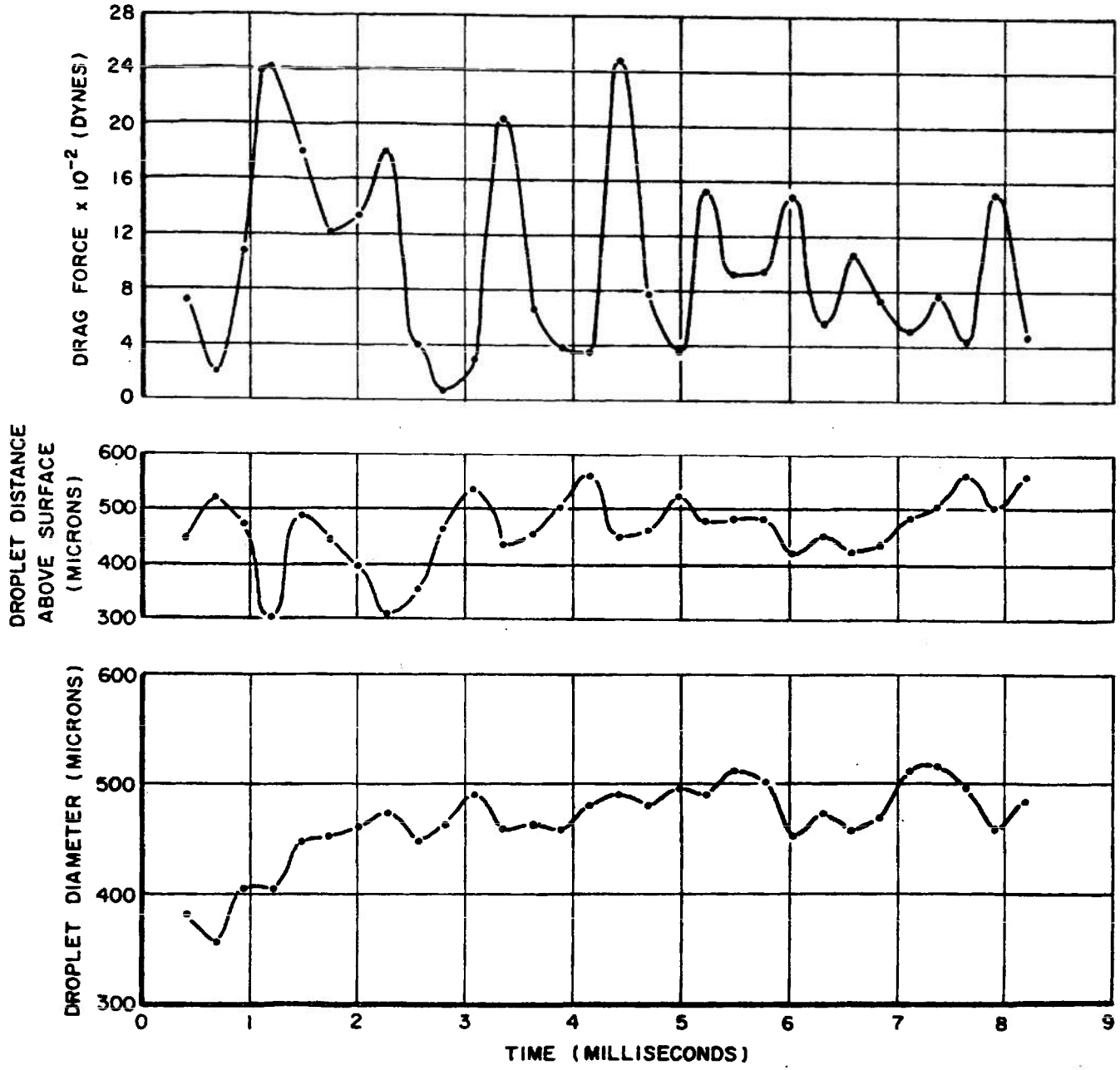


Figure 11. Measured diameters of a single droplet and distances above the propellant surface together with computed drag forces plotted vs. time. The measured values were determined during the period of droplet growth. Run 444, Propellant = Lot 225, Chamber Pressure = 500 psi.

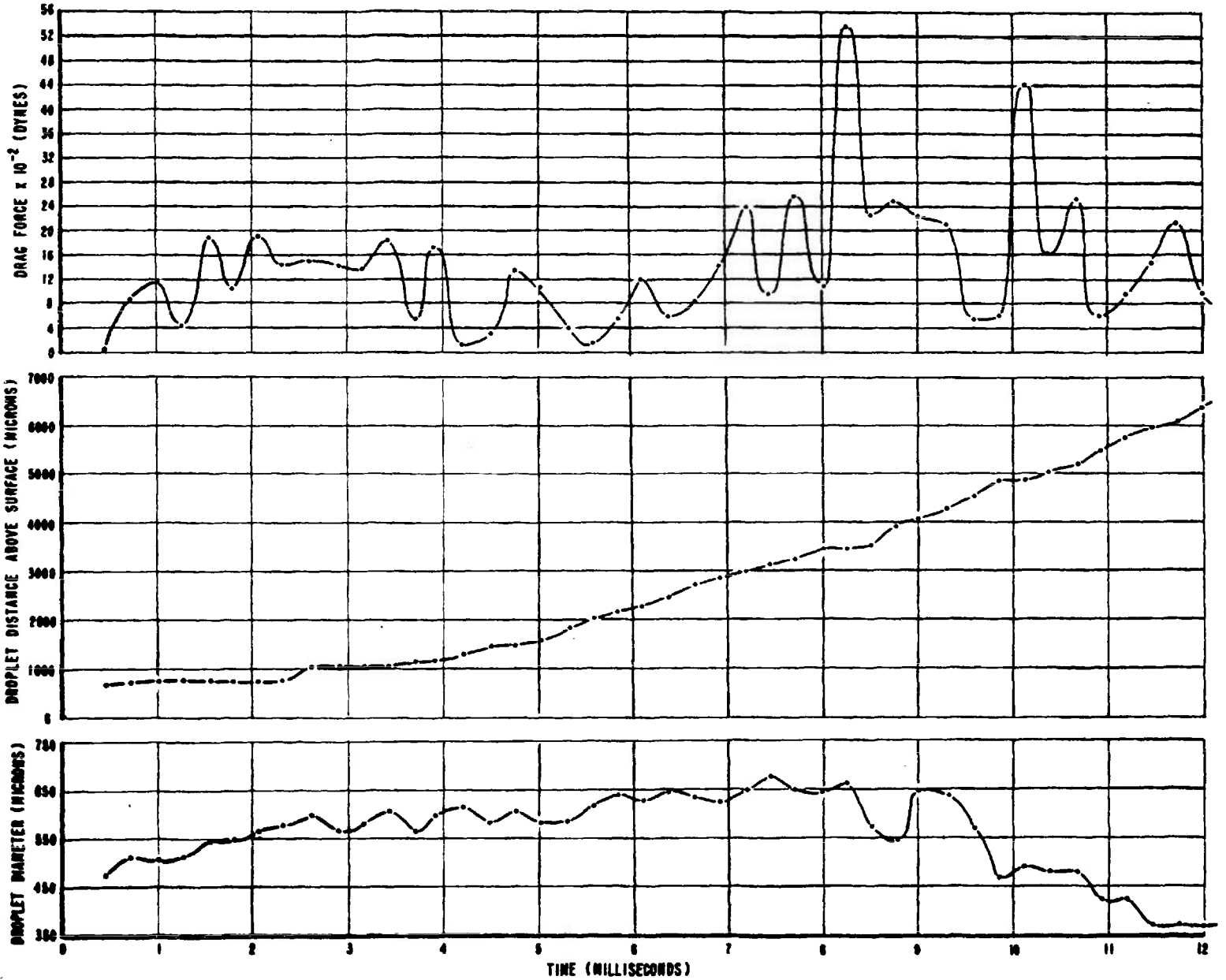


Figure 12. Measured diameters of a single droplet and distances above the propellant surface together with computed drag forces plotted vs. time. The measured values were determined from the same droplet that was followed in Figure 11 but at a later time (as average diameter decreased). Run 444, Propellant = 225. Chamber Pressure = 500 psi.

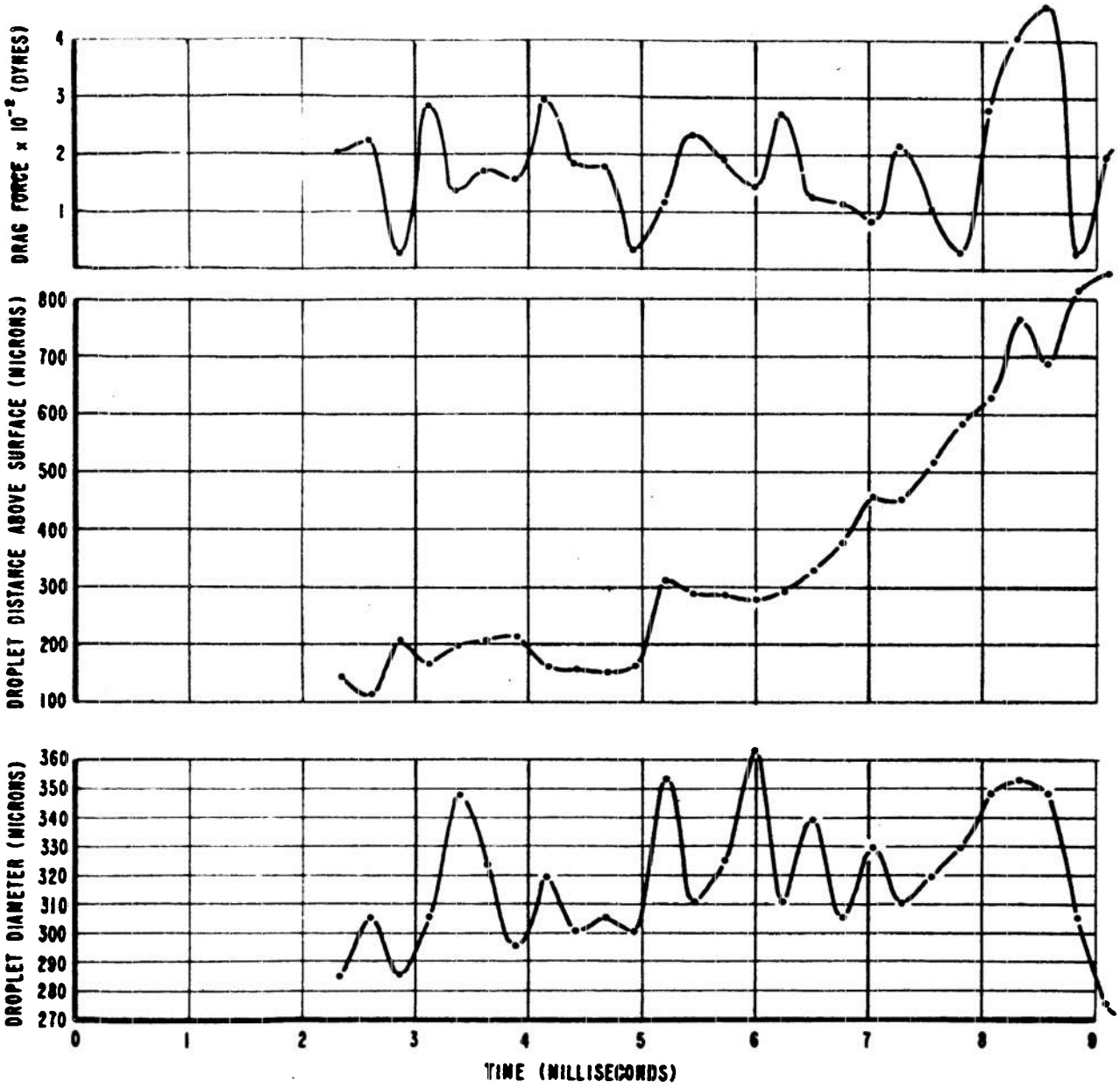


Figure 13. Measured diameters of a single droplet and distances above the propellant surface together with computed drag forces plotted vs. time. The measured values were determined as the average diameter reached a maximum. Run 463, Propellant = Lot 228, Chamber Pressure = 325 psi.

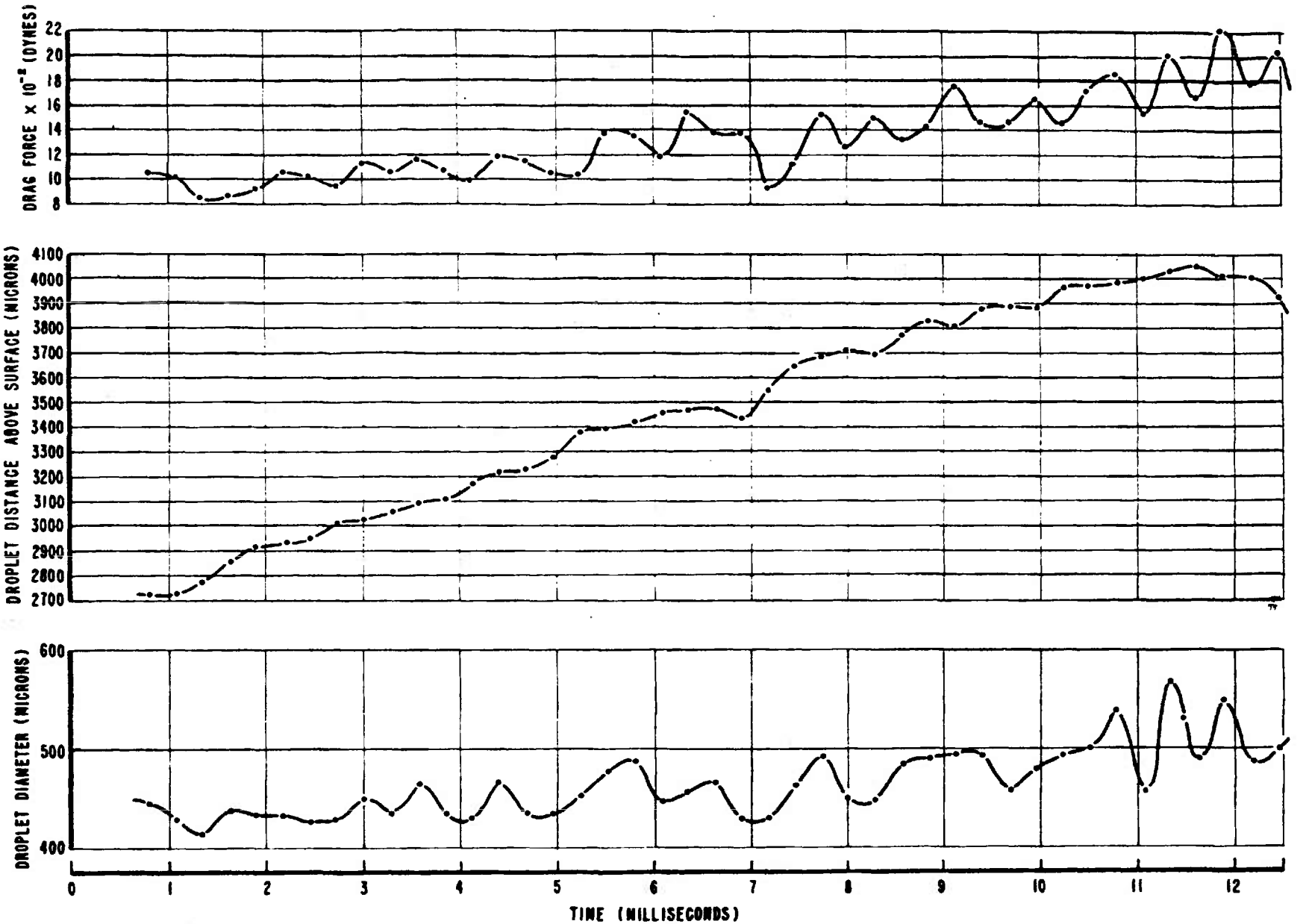


Figure 14. Measured diameters of a single droplet and distances above the propellant surface together with computed drag forces plotted vs. time. The measured values were determined during the period of droplet growth. Run 469, Propellant = Lot 225, Chamber Pressure = 225 psi.

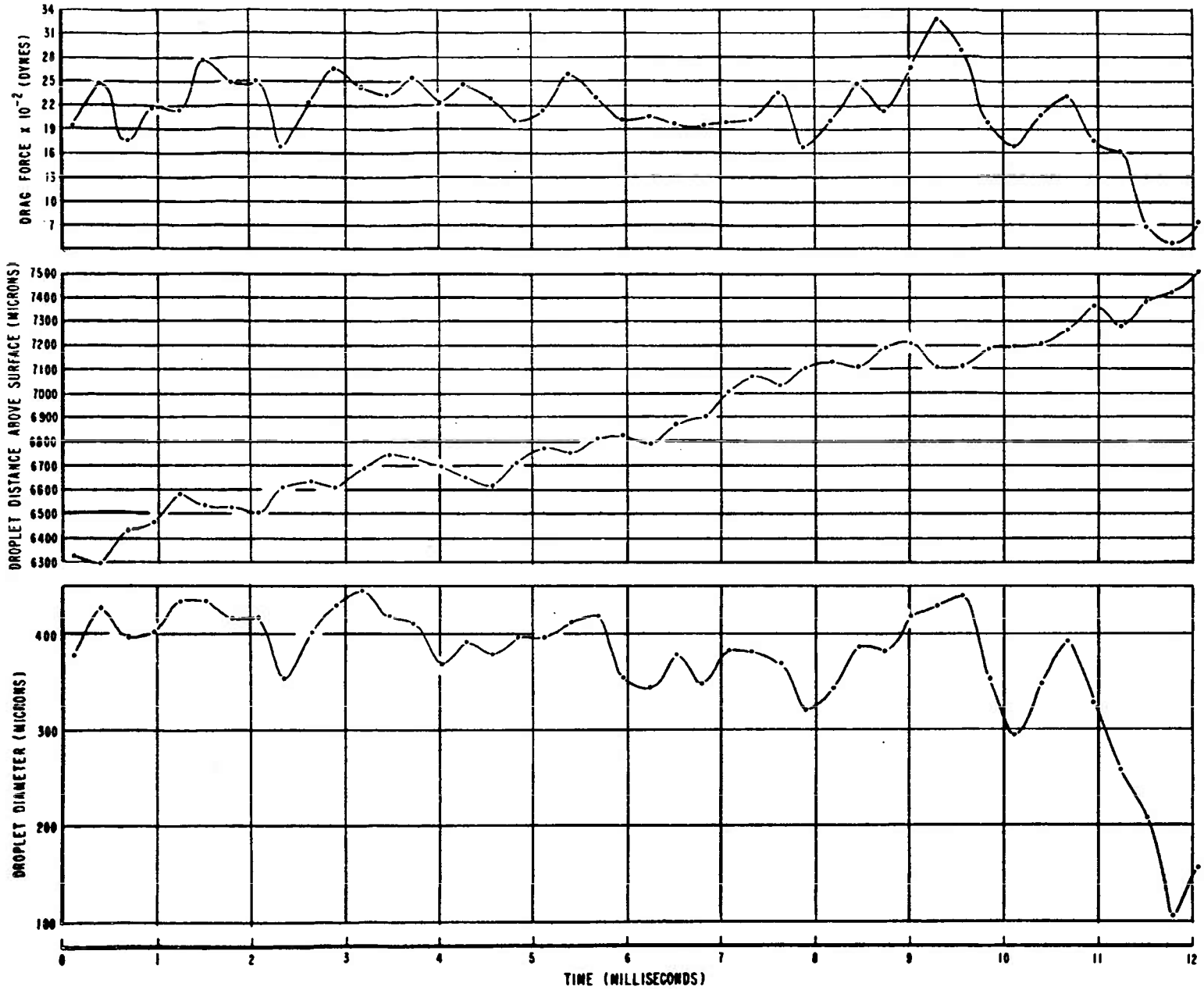


Figure 15. Measured diameters of a single droplet and distances above the propellant surface together with computed drag forces plotted vs. time. The measured values were determined during the decay period of the same droplet traced in Figure 14. Run 469, Propellant = lot 225, Chamber Pressure 225 psi.

Figure 16 is a plot summarizing the data obtained on lots 223, 224 and 225. It shows the percentage of particles in a thin zone above the surface with diameters in the same range as the original particle sizes. The percentage is shown as a function of pressure and aluminum concentration in the propellant. The percentage of particles with diameters greater than the original particle size is highest at the low pressures and high aluminum concentrations in the propellants. This phenomena, we believe, is an indication of the amount of agglomeration and meteoric pelting taking place in the thin zone next to the surface. Apparently at high pressures and low initial aluminum concentrations, the opportunity for agglomeration or pelting after the aluminum melts is reduced.

Some measurements made in thicker zones above the surface are shown in figure 17. In general these findings verify those made in zones near the surface by reflecting the results of phenomena that have occurred there.

Aluminum mass flux determinations were made based on visible particles in the motion pictures. The framing rate was such that most larger droplets were essentially stopped for frame to frame measurements. A fairly accurate determination of the velocities of the various sized droplets could then be made. The simple relationship was used of

$$\text{Total Mass Flux} = \sum m_i \, v_i$$

where $m_i$ and $v_i$ were the total mass and velocity of the $i^{th}$ species, respectively.

In most instances mass flux variations of a low frequency nature (300-700 cps) were observed in the thin zones above the surface. Figures 18 and 19 show plots of aluminum mass flux vs. time for propellant containing 20 per cent of aluminum (lot 225). These plots represent firings at two different chamber pressures of 300 and 500 psi. The variations were often quite large but the mean value was lower than the calculated aluminum mass evolution rate from the

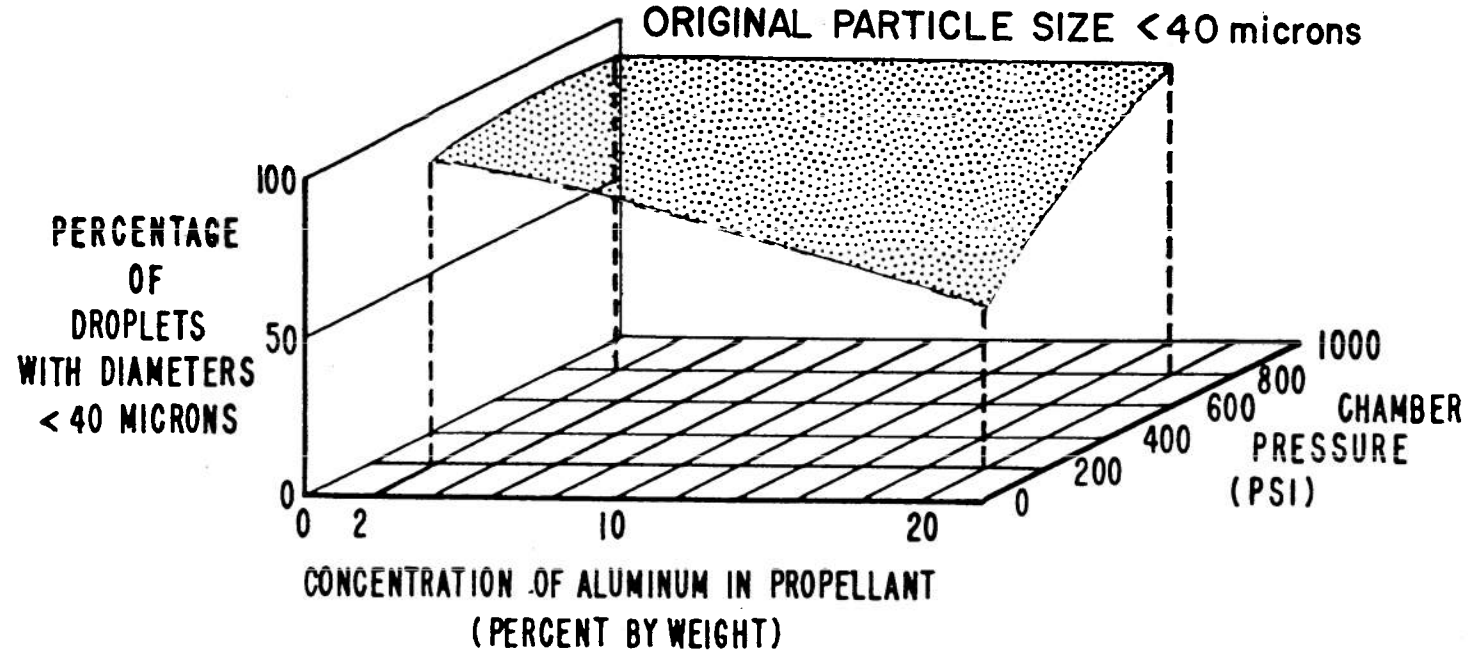


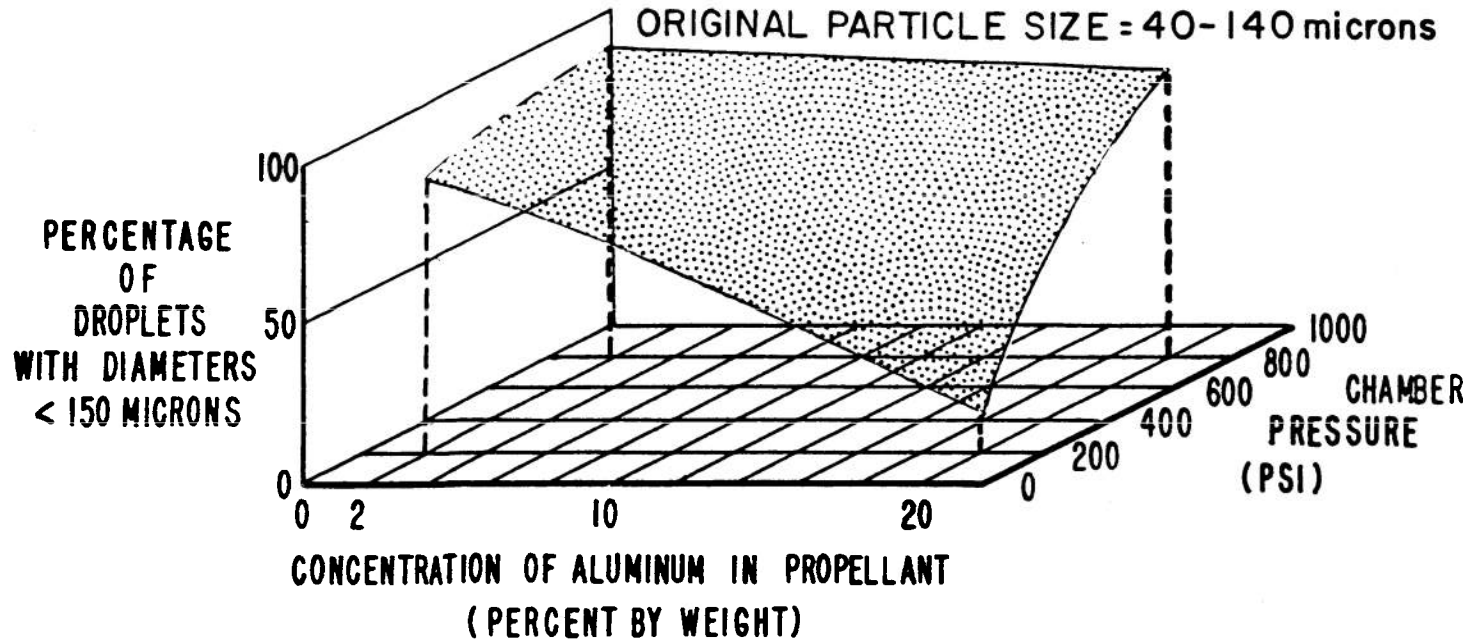


Figure 16. Plot of percentage of particles with diameters in the same range as the original particle sizes. Measurements were made in a zone 200 microns in height above the burning surface of the propellant. This is plotted as a function of pressure and concentration. Propellants represented are lots 223, 224 and 225.

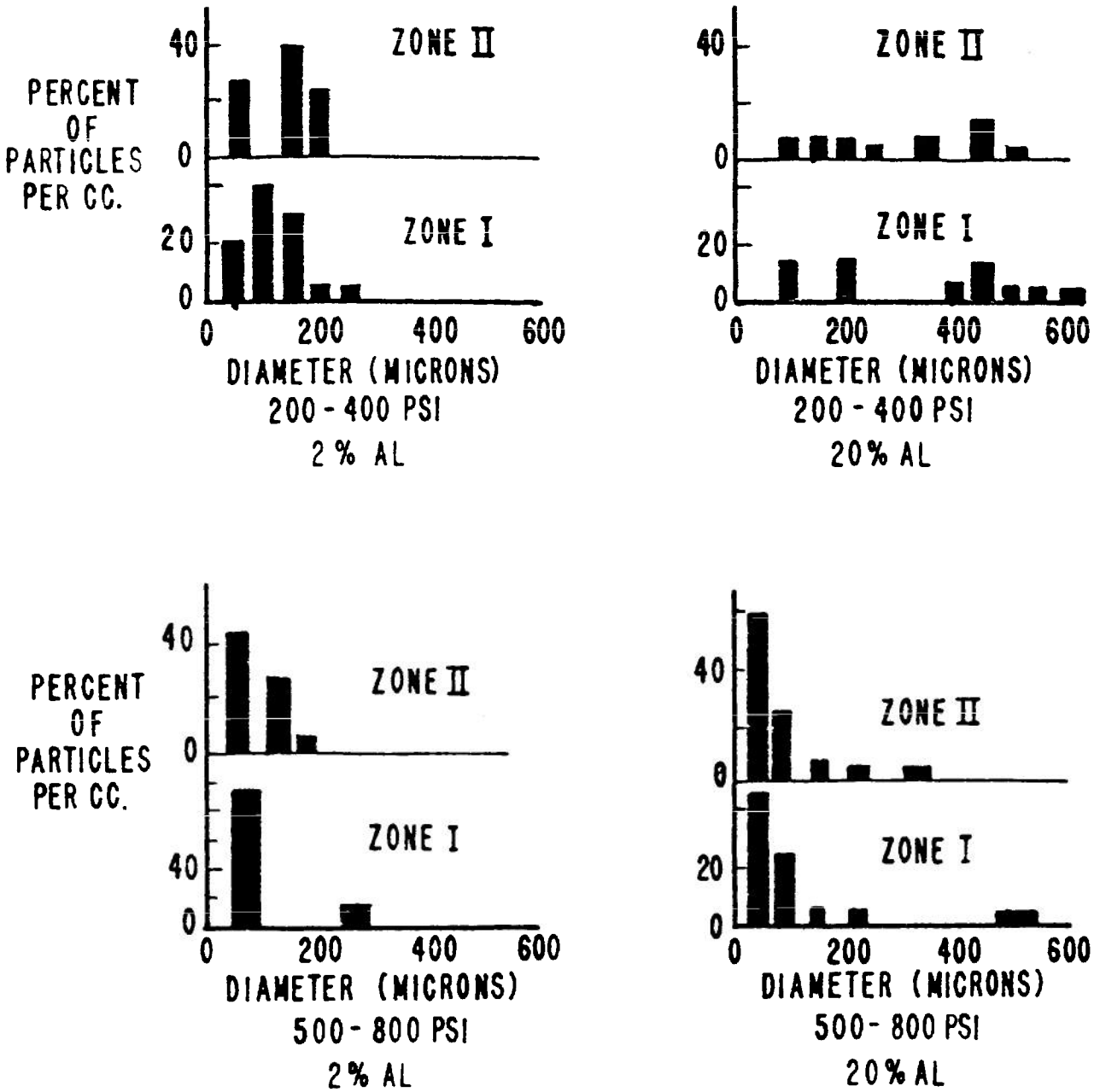


Figure 17. Plots of particle diameters and concentrations in thick zones above the propellant surfaces. They are shown as a function of pressure and initial aluminum concentration. ZONE I = 1750 microns high; ZONE II = 3500 microns high.

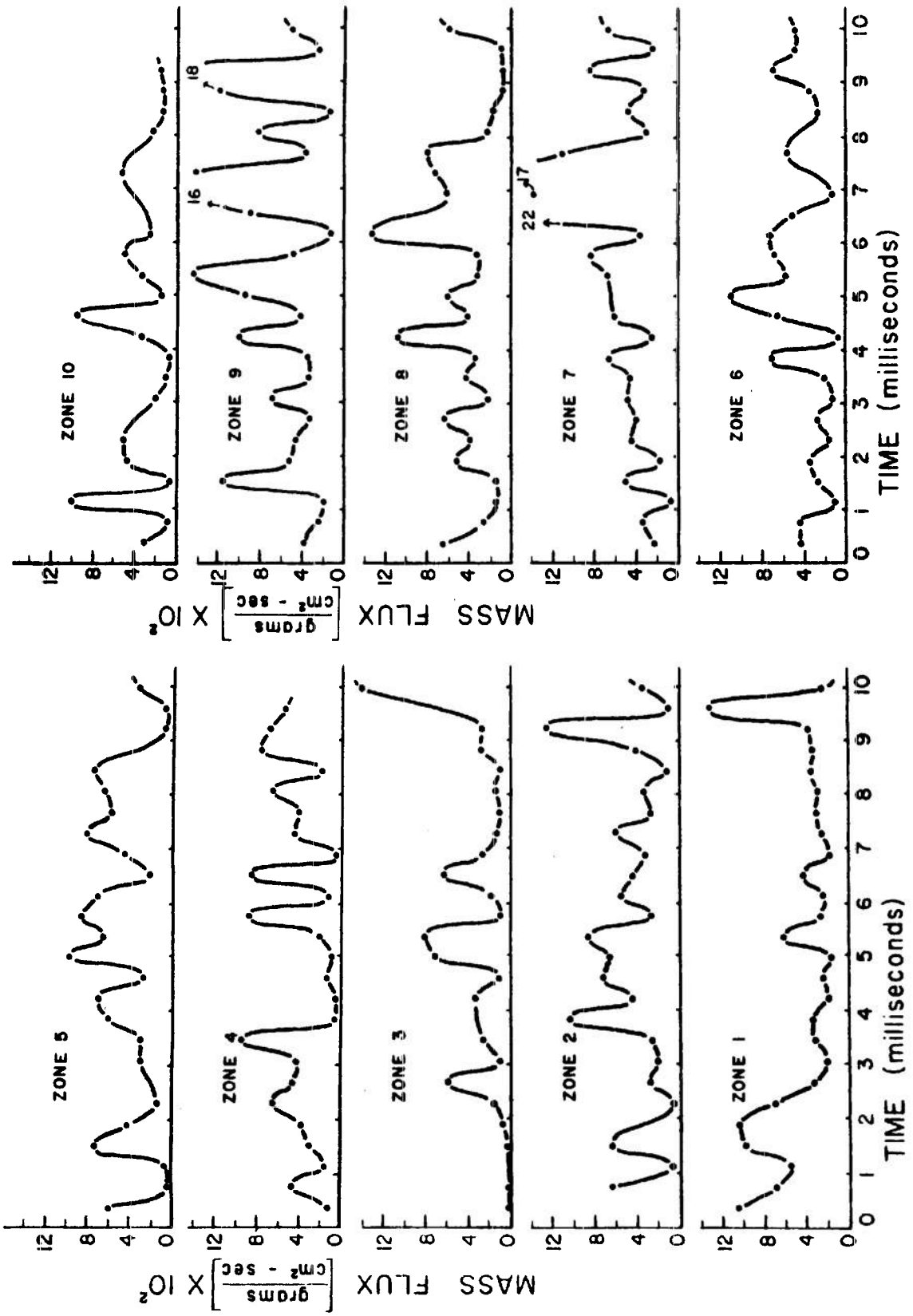


Figure 18. Plot of aluminum mass flux vs. time in 10 zones projecting upwards from the propellant surface. Each zone is 190 microns in height. Chamber Pressure = 300 psi. Propellant = lot 225.

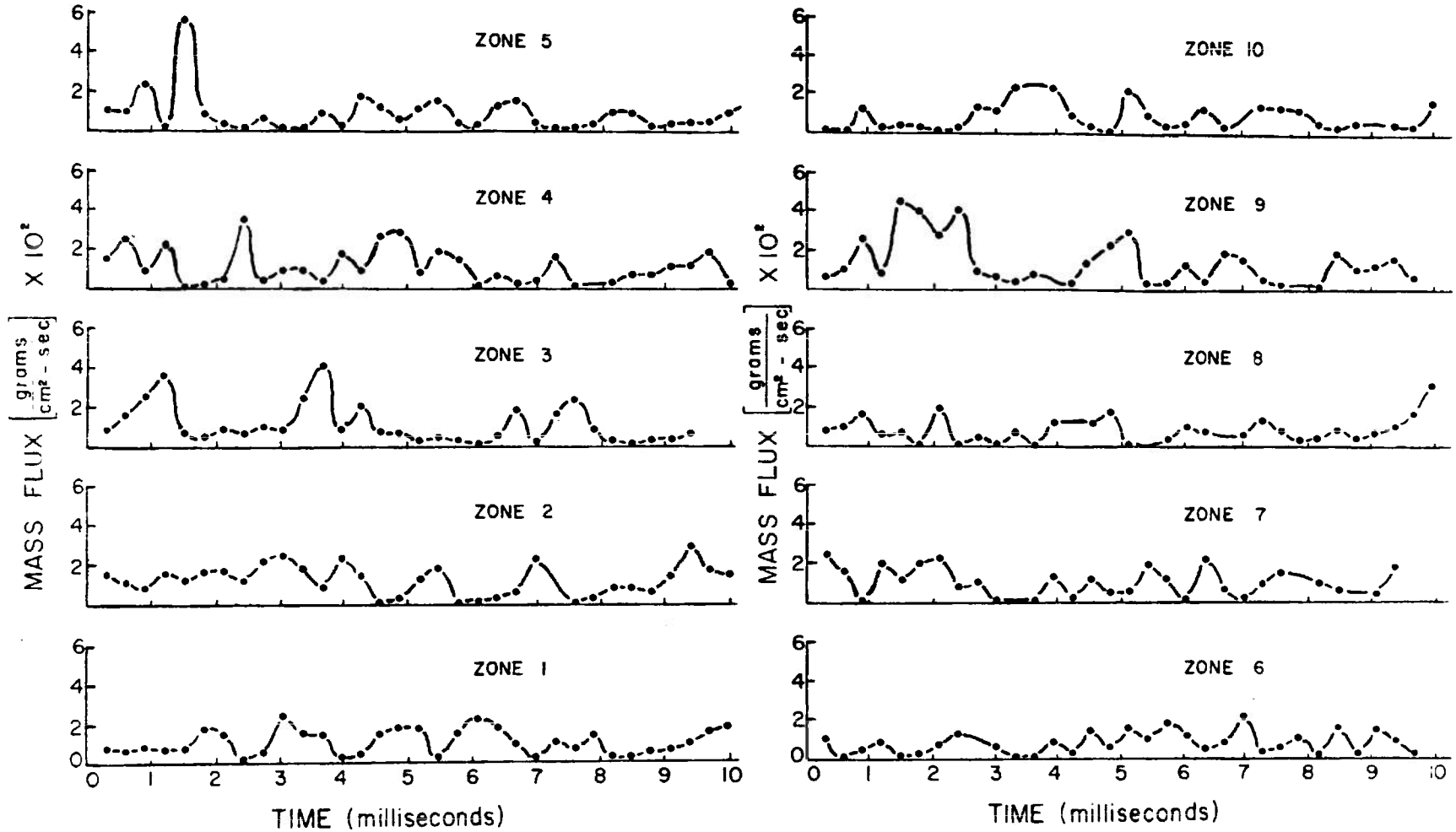


Figure 19. Plot of aluminum mass flux vs. time in 10 zones projecting upwards from the propellant surface. Each zone is 190 microns in height. Chamber Pressure = 500 psi. Propellant = lot 225.

propellant surface. This discrepancy is to be expected since all of the aluminum particles are not visible on the film. The important factor brought out by these measurements is not the absolute values of the burning particle flux (probable error $\pm$ 10 per cent) but the fact that it is varying significantly at a low frequency. This phenomena may be a key point in luminosity variations reported by other investigators[8].

## 4. CONCLUSIONS

The following conclusions are drawn from the experimental results:

(1) Agglomeration of aluminum on the burning surface of a double base - composite propellant is appreciable. It appears to be a function of chamber pressure and initial aluminum concentration in the propellant. In cases observed where it almost covers the surface as a molten blanket, it would probably alter the acoustic admittance of the burning surface.

(2) The vibration or oscillation of liquid droplets above the propellant burning surface is a measurable phenomenon. It is concluded that even though the majority of the droplets measured were vibrating in the low frequency range ($<$ 1000 cps), this is not a major contributor to low frequency pressure oscillations. Concentration profiles taken above the surface support this postulate.

(3) Most of the droplets in zones up to 3.5 mm thick above the propellant surfaces were apparently liquid rather than hollow spheres with liquid walls.

(4) Measurements show that appreciable droplet evaporation or burning may occur at a relatively large distance above the surface. It is postulated that this is a vapor controlled process. Siren pulsation increased the evaporation rate of the droplets but did not affect the distance above the surface at which it became controlling.

(5) The mass flux of aluminum above the propellant surface varied with time at a low frequency. It is concluded that this could be a major contributor to low frequency chamber oscillations measured in some highly aluminized propellant systems.


## ACKNOWLEDGMENTS

The authors are indebted to Mr. Richard Strittmater, Mr. Eugene Bonhage, Dr. Richard Jones, and Mr. James Cole of the Interior Ballistics Laboratory for their help and discussions during the course of this program.


Leland A. Watermeier

LELAND A. WATERMEIER

William P. Aungst

WILLIAM P. AUNGST

S. P. Pfaff

SAMUEL P. PFAFF

## REFERENCES


1. Summerfield, M.: Solid Propellant Rocket Research, Academic Press, 1, pp. 253-291, (1960).

2. Watermeier, L.: "An Experimental Study of Combustion Instability in Solid Rocket Propellants - Part II", Ballistic Research Laboratories Report 1116 (Sept. 1960) and ARS Journal, 31, pp. 564-566 (1961).

3. Baer, P., Geene, R., Smith, H. and Wortman, J.: Propellant Thermodynamic Performance Calculations For Rocket Engines, Proceedings of First Conference on Kinetics, Equilibria and Performance of High Temperature Systems, Butterworth and Co. Limited, pp. 90-104 (1959).

4. Burgoyne, J. and Cohen, L.: Proceedings of Royal Society, A-225, 375-392 (1954).

5. Lord Rayleigh: Theory of Sound, II, 373, (1945).

6. Morse, P. and Feshbach, H.: Methods of Theoretical Physics, Part II, 1470, McGraw-Hill Book Co., Inc. (1953).

7. Dodge, R. A. and Thompson, M. J.: Fluid Mechanics, McGraw-Hill Book Co., Inc., 337-38, (1937).

8. Shanfield, H., et al: "Study of Resonance Behavior in Solid Propellants", Quarterly Reports, NAVORD Contract 17945, task 2, Aeroneutronics (1961-1962).

9. Miesse, C. C.: "Ballistics of an Evaporating Droplet," Jet Propulsion 24, No. 4, 237-244 (July 1954).

10. Schuyler, F. L.: "Combustion Instability; Liquid Stream and Droplet Behavior - Part I, Experimental and Theoretical Analysis of Evaporating Droplets," WADC Technical Report 59-720 (September, 1960).

11. Goldsmith, M. and Penner, S.S.: "On the Burning of Single Drops of Fuel in an Oxidizing Atmosphere," Jet Propulsion 24, No. 4, 245-251 (July, 1954).

12. Godsave, G.A.E.: Studies of the Combustion of Drops in a Fuel Spray - The Burning of Single Drops of Fuel. Fourth International Symposium on Combustion, p. 823. Baltimore, The Williams and Wilkens Co. (1953).

13. Ranz, W. E. and Marshall, W. R., Jr.: "Evaporation from Drops," Chemical Engineering Progress, 48, 141-146, 173-180 (1952).

Page intentionally blank

Page intentionally blank

Page intentionally blank

# A P P E N D I C E S

Page intentionally blank

Page intentionally blank

Page intentionally blank

## APPENDIX I

## DROPLET EVAPORATION RATE IN A FLOWING MEDIUM

In an effort to analyze data of the type presented in Table 3, a treatment was used which is based on fundamental work done on liquid droplet burning or evaporation. A modification of the analytical approach presented by Miesse[9], Schuyler[10], Goldsmith and Penner[11] was used. The following assumptions were made as simplifying factors: (1) the spheres or droplets are molten aluminum droplets burning (evaporating) in a hot flowing, propellant product gas atmosphere; (2) the droplets leave the propellant surface at approximately the same velocity as the product gases (drag effects take over at some distance above the surface); (3) each burning droplet is surrounded by a halo or glow which is very nearly the same diameter as the droplet and which varies proportionately with the droplet diameter; (4) the velocity of the product gases increases linearly with distance above the propellant surface; (5) the gaseous flow around the droplet is laminar in all instances where no siren pulses were introduced; and (6) the burning or evaporation rate of the droplet is diffusion controlled.

Newton's second law provides the means for expressing velocity, mass, and force relationships for spherical droplets,

$$\frac{dv}{dt} = a + \frac{F}{M} \tag{1}$$

By expressing the mass of a droplet, M, as $\pi\rho' D^3/6$, then,

$$\frac{dv}{dt} = a + \frac{6F}{\pi\rho' D^3} \tag{2}$$

The drag force, F, can be represented by,

$$F = C_D \ \pi D^2 \rho \ (V_p - v)^2/8 \tag{3}$$

If the drag coefficient of a solid sphere is considered in the following form,

$$C_D = \frac{24}{R_e} = 24\nu/ (V_p - v) D \tag{4}$$

which is valid for laminar flow with small Reynolds numbers, then substituting equations (3) and (4) into (2) yields

$$\frac{dv}{dt} = a + \left[ k \frac{(V_p - v)}{D^2} \right] \tag{5}$$

The viscosity parameter, k, is equal to $18\mu/\rho'$ with $\mu$ being the dynamic viscosity of the product gases. Godsave[12], Ranz and Marshall[13] have found experimentally that droplet diameter and evaporation rate bear the relation

$$D^2 = D_o^2 - \lambda t \tag{6}$$

where $D_o$ represents the initial diameter of the droplet and $\lambda$ is the droplet evaporation rate. It was illustrated by Miesse that the value of $D^2$ was linear with time for droplet diameters of 400 microns or larger. It was assumed that this linear relationship held for all of the droplets studied in this investigation regardless of size.

A series solution used by Schuyler was first relied upon to obtain the equations needed as a basis for our studies. This solution gives an idea of the initial diameter of an aluminum droplet which would just completely evaporate at a specified distance above the propellant surface. This distance was arbitrarily chosen as approximately 1.6 cm.*

The Series Solution. If we substitute equation (6) and $W = D^2$ into equation (5) we get

*The value of 1.6 cm was used because, in the limit, this was approximately the distance above the propellant surface visible in the motion picture frames. Also, that distance would encompass the reaction zone as well as a large portion of the so-called flame zone.

$$\frac{W\,dv}{dW} = q\,(v - V_p) - \frac{aW}{\lambda} \tag{7}$$

where $q = k/\lambda$. A dimensionless term, r, can be defined as

$$r = \frac{V_L - V'_p}{L\lambda}\,W \tag{8}$$

By substituting equation (8) into (7), letting $a = 0$, and differentiating with respect to r, we obtain

$$r\frac{d^2v}{dr^2} + (1-q)\frac{dv}{dr} = qv \tag{9}$$

Assuming $v = \sum_{m=o}^{\infty} C_m\, r^{p+m}$, we find that $p = 0$ and $p = q$. By letting $p_1 = 0$ and $p_2 = q$, the following is obtained

$$v = r^{p_1}\sum_{m=o}^{\infty} a_m\, r^m + r^{p_2}\sum_{m=o}^{\infty} b_m\, r^m \tag{10}$$

Solving for $a_m$ and $b_m$,

$$a_m = \frac{q^m\, a_o}{m!\,(m-q)!^*}\;;\quad (m-q)!^* = (m-q)(m-1-q)\;\text{---}(1-q) \tag{11}$$

$$b_m = \frac{q^m\, b_o}{m!\,(m+q)!^*}\;;\quad (m+q)!^* = (m+q)(m-1+q)\;\text{---}(1+q) \tag{12}$$

By substituting equations (11) and (12) into (10) and simplifying,

$$v = a_o + \sum_{m=1}^{\infty}\frac{q^m\, a_o\, r^m}{m!\,(m-q)!^*} + r^q\left[b_o + \sum_{m=1}^{\infty}\frac{q^m\, b_o\, r^m}{m!\,(m+q)!^*}\right] \tag{13}$$

The following boundary conditions are applied to find $a_o$ ($= V_{L,cal}$), $r = o$ (when $D = o$) and $v = V_{L,cal}$; to find $b_o$ ( = some quantity. $V_{L,cal}$), $r = r_o$ and $v = v_o$.

Equation (13) then becomes,

$$\frac{v}{V_{L,cal}} = 1 + \sum_{m=1}^{\infty} \frac{q^m r^m}{m!(m-q)!*} + \left\{ \frac{\frac{v_o}{V_{L,cal}} - 1 - \sum_{m=1}^{\infty} \frac{q^m r_o^m}{m!(m-q)!*}}{r_o^q + \sum_{m=1}^{\infty} \frac{q^m r_o^{m+q}}{m!\,(m+q)!*}} \right\} \left\{ r^q + \sum_{m=1}^{\infty} \frac{q^m r^{m+q}}{m!\,(m+q)!*} \right\} \qquad (14)$$

Integrating equation (14) and using the boundary condition $X = L_{cal}$, $r = o$ (when $D = o$) gives

$$\left(1 - \frac{X}{L,cal}\right)\left(1 - \frac{V_p'}{V_{L,cal}}\right) = r + \sum_{m=1}^{\infty} \frac{q^m r^{m+1}}{(m+1)!*(m-q)!*} + \left( \frac{\frac{v_o}{V_{L,cal}} - 1 - \sum_{m=1}^{\infty} \frac{q^m r_o^m}{m!(m-q)!*}}{r_o^q + \sum_{m=1}^{\infty} \frac{q^m r_o^{m+q}}{m!\,(m+q)!*}} \right) \left( \frac{r^{q+1}}{q+1} + \sum_{m=1}^{\infty} \frac{q^m r^{m+q+1}}{m!\,(m+q+1)!*} \right)$$

---------- (15)

The value of $D_{o\ MAX}$ can be found by applying $\frac{X}{L,cal} = 0$ and $r = r_o$ to equation (15);

$$\frac{1 - \frac{V_p}{V_{L,cal}} - r_o - \sum_{m=1}^{\infty} \frac{q^m r_o^{m+1}}{(m+1)!*(m-q)!*}}{\frac{r_o^{q+1}}{q+1} + \sum_{m=1}^{\infty} \frac{q^m r_o^{m+q+1}}{m!(m+q+1)!*}} = \frac{\frac{v_o}{V_{L,cal}} - 1 - \sum_{m=1}^{\infty} \frac{q^m r_o^{m}}{m!(m-q)!*}}{r_o^{q} + \sum_{m=1}^{\infty} \frac{q^m r_o^{m+q}}{m!(m+q)!*}} \qquad \text{---------- (16)}$$

Then $r_o = r_{o\ MAX.}$ can be found from equation (16). Once $r_{o\ MAX.}$ and its corresponding value for the right hand term of equation (16) are found, the rest of the droplet's history is easily obtained.

The Revised Solution. The series solution is, of course, a very specific treatment. In our experiments we were concerned with droplets which could either completely evaporate before $\frac{X}{L} = 1$ (less than 1.6 cm above propellant surface) or after $\frac{X}{L} = 1$. Therefore, the following approach was used. We will consider a model in which the propellant product gas velocity, $V_p$, can be represented as linearly increasing above the propellant surface (see sketch below).

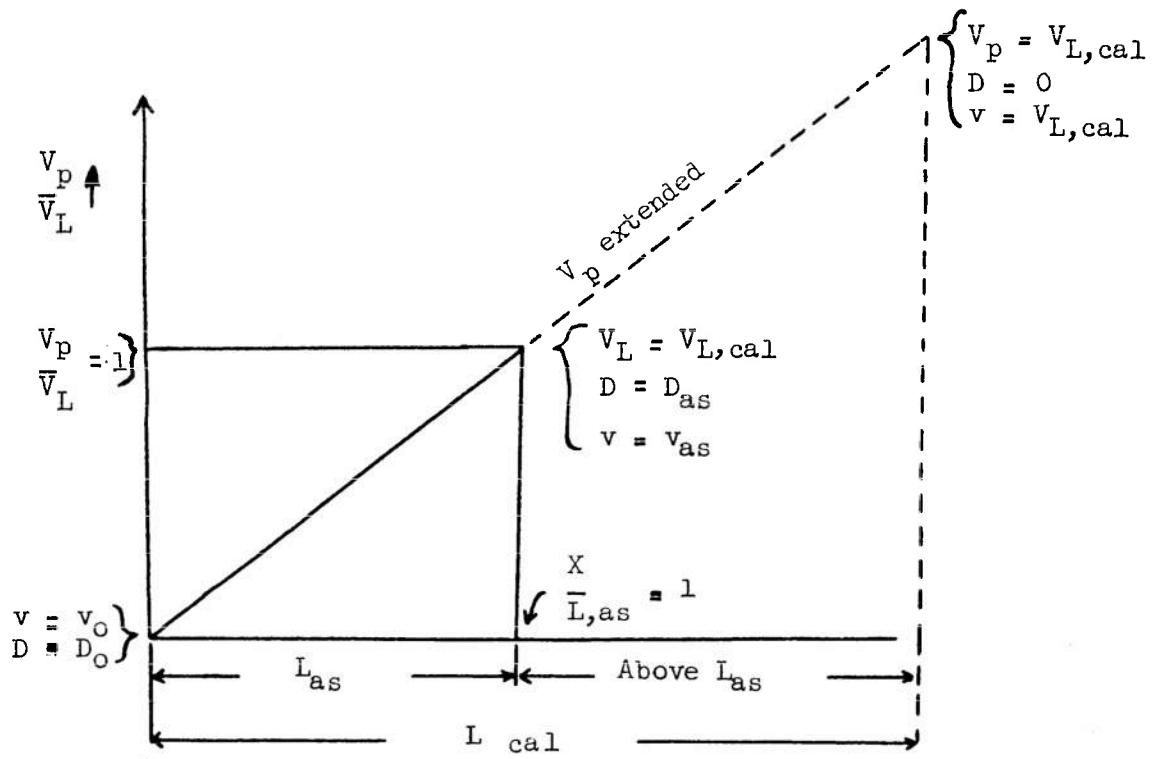

This straight line is extended beyond the designated distance above the surface ($L_{as}$) which is the case if $D_o > D_{o,MAX}$. A point will be reached at which the droplet with $D_o$ of interest will completely evaporate or burn. The gas velocity at that point is $V_p = V_{L,cal} > V_{L,as}$ and the corresponding distance above the propellant surface is $X = L_{cal} > L_{as}$.

The value of $V_p$ is determined by using equation (16) of the series solution which allowed determination of $D_{o\ MAX}$ for a particular $V_L$ and $v_o$.

From equation (16), it is seen that if $v_o$, $D_o$, and $r_o$ are known, the value of $V_{L,cal}$ can be obtained. Once the $V_L = V_{L\ cal}$ and its corresponding $X = L_{cal}$ are obtained, they are used in the boundary conditions for equations (14) and (15), as the $V_L$ and L for which $D = 0$. We are interested, however, only in the droplet's history up to $X = L_{as}$. Therefore it is necessary to find the diameter, $D = D_{as}$, corresponding to $\frac{X_{as}}{L_{cal}} = \frac{L_{as}}{L_{cal}}$. This value, $D_{as}$ corresponding to $r_{as}$, is then put into equation (14) so that $\frac{v}{V_{L\ cal}} = \frac{v_{as}}{V_{L\ cal}}$ can be be determined.

After $\frac{v_{as}}{V_{L\ cal}}$, $\frac{X_{as}}{L\ cal} = \frac{L_{as}}{Lcal}$, and $D = D_{as}$ have been found, the determination of the rest of the aluminum droplet's history is routine. Therefore, using Schuyler's method, we can approximate any particular droplet's history as it travels away from the surface.

## LIST OF SYMBOLS

CGS Units

$a$ = gravitational acceleration of droplet

$C_D$ = drag coefficient

$D$ = droplet diameter at any time, cm.

$D_o$ = initial droplet diameter, cm.

$D_{o,MAX}$ = maximum initial droplet diameter, cm.

$D_{as}$ = diameter of droplet at distance $L_{as}$ above surface, cm.

$F$ = drag force, dynes

$k$ = viscosity parameter, $18\mu/\rho'$

$L$ = distance above surface at any time, cm.

$L_{cal}$ = calculated distance above surface, cm.

$L_{as}$ = distance above surface (reference), cm.

$M$ = mass of droplet, gms. = $\pi\rho' D^3/6$

$m$ = number of droplets (unity for this program)

$q$ = $k/\lambda$

$Re$ = Reynolds number = $|V_p - v|D/\nu$

$r$ = $\dfrac{V_L - V_p' W}{L\lambda}$ (dimensionless)

$r_o$ = value of r using $D_{o\ MAX}$ conditions

$t$ = time, sec.

$v$ = droplet velocity, cm/sec.

$v_o$ = initial droplet velocity, cm/sec.

$v_{as}$ = velocity of droplet at reference distance above surface, cm/sec.

$V_L$ = product gas velocity at X = L, cm/sec.

$V_{L,cal}$ = calculated product gas velocity, cm/sec.

$V_{L,as}$ = product gas velocity at reference distance above surface, cm/sec.

$V_p$ = product gas velocity at any distance above surface, cm/sec.

$V_p'$ = product gas velocity at the surface, cm/sec.

$W$ = $D^2$, $cm^2$

$X$ = distance above surface, cm.

$X_{as}$ = distance to reference point above surface, 1.6 cm.

$\rho$ = product gas density, gm/cc.

$\rho'$ = droplet density, gm/cc.

$\nu$ = kinematic viscosity of product gases, $\mu/\rho$

$\mu$ = dynamic viscosity of product gases, dynes-sec/$cm^2$

$\lambda$ = evaporation rate of droplet in still atmosphere, $cm^2$/sec.

## APPENDIX II

## PROPERTIES OF LIQUID ALUMINUM USED IN CALCULATIONS

The following properties of aluminum (liquid) were used for computational purposes. They were obtained from metals handbooks or other references.*

### Surface Tension

The values of the surface tension as a function of temperature are plotted in figure A. No values were used beyond the boiling point temperature although it is assumed that liquid aluminum droplets would have a finite lifetime if injected into a medium whose temperature exceeded the boiling point.

### Density

Reference books give values of aluminum density varying from 2.7 at 293°K to 2.261 at 1373°K. The value of 2.2 was used in this investigation as a fair estimate of that encountered throughout the temperature range involved.

### Evaporation Rates of Aluminum in Still Atmosphere, $\lambda$.

The following equation is given by Kennard for maximum rate of evaporation;

$$G = \frac{\gamma p}{\sqrt{2\pi R_G T}}$$

where G = maximum rate of evaporation $\frac{\text{gms}}{\text{cm}^2\text{-sec}}$, $\gamma$ = coefficient of evaporation (assumed unity), p = vapor pressure in dynes/$\text{cm}^2$, $R_G = \frac{R}{M} = 3.08 \times 10^6$, T = °K.

---

*Smithells, C.J.: Metals Reference Book, Volume 2, Butterworths Scientific Publications (1955)

Avco Corp.: The Vaporization and Physical Properties of Certain Refractories. Quarterly Summary Report No. 5, May, 1961.

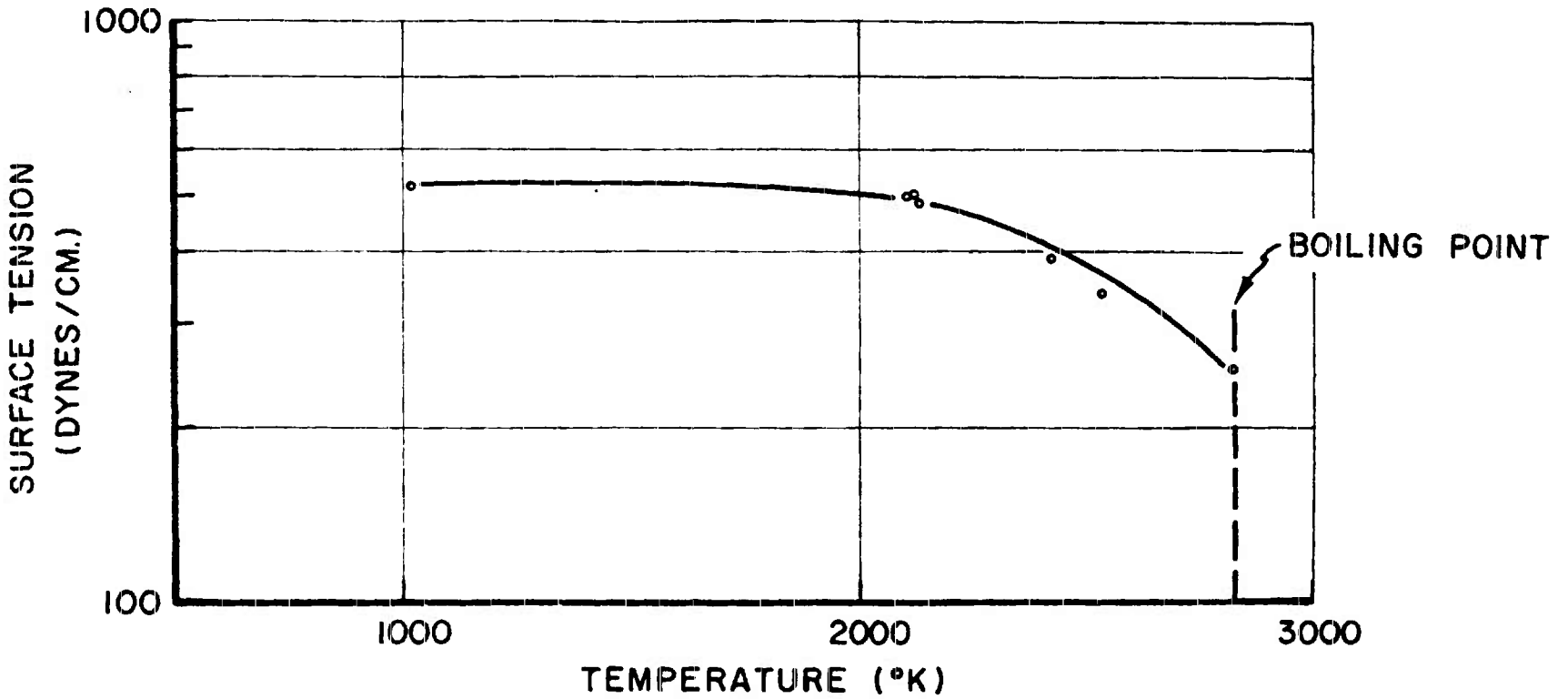


Figure A. Surface tension as a function of temperature for pure liquid aluminum.

The evaporation rate, $\lambda$, as defined in reference 6 is,

$$\lambda = \frac{d(D^2)}{dt} = 2D \frac{dD}{dt}, \quad \text{units} = cm^2/sec.$$

Therefore, the following relationship can be derived

$$G = \frac{\rho\lambda}{4D}.$$

Vapor Pressure

The vapor pressure of liquid aluminum was computed using the following equation which is supposedly good in the 1200 to 2800°K range;

$$\log p = -\frac{A}{T} + B + C \log T$$

where $A = 1.645 \times 10^4$, $B = 12.36$, $C = -1.023$, $p$ = vapor pressure, mm. Hg., and $T = {}^{o}K$.

Page intentionally blank

Page intentionally blank

Page intentionally blank

DISTRIBUTION LIST

| No. of Copies | Organization |
|---|---|
| 3 | Director<br>National Aeronautics & Space Administration<br>Lewis Research Center<br>ATTN: Dr. A.E. Potter, Jr.<br>Dr. L.A. Povinelli<br>Dr. C.C. Ciepluch<br>Cleveland Airport<br>Cleveland, Ohio |
| 1 | AeroChem Research Laboratories, Inc.<br>ATTN: Dr. H.F.Calcote<br>P. O. Box 12<br>Princeton, New Jersey |
| 1 | Armour Research Foundation<br>ATTN: Dr. Fred Schuyler<br>Illinois Institute of Technology Center<br>Chicago 16, Illinois |
| 1 | CONVAIR, A Division of General Dynamics Corporation<br>Convair Scientific Research<br>ATTN: Dr. A.L. Berlad<br>San Diego, California |
| 1 | Ford Motor Company<br>Aeronutronic Division<br>ATTN: Dr. Richard Hoglund<br>Mgr., Fluid Mechanics Dept.<br>Ford Road<br>Newport Beach, California |
| 3 | Thiokol Chemical Corp.<br>Elkton Division<br>ATTN: Dr. Ernest Sutton<br>Mr. Gene Pacanowsky<br>Mr. Edward Sterne<br>Elkton, Maryland |
| 50* | Applied Physics Laboratory<br>The Johns Hopkins University<br>ATTN: Dr. Walter G. Berl<br>8621 Georgia Avenue<br>Silver Spring, Maryland |
| 1 | University of Illinois<br>College of Engineering<br>ATTN: Dr. Roger Strehlow<br>Department of Aeronautical Engineering<br>Urbana, Illinois |
| 1 | Stanford Research Institute<br>ATTN: Dr. George Agoston<br>Poulter Laboratories<br>Menlo Park, California |
| 123 | Joint Army-Navy-Air Force Solid Propellant Mailing List dated June 1961 |

* For distribution to SPIC Panel.

AD _____ Accession _____

Ballistic Research Laboratories, APG

AN EXPERIMENTAL INVESTIGATION OF POSSIBLE ALUMINUM ADDITIVE CONTRIBUTIONS TO UNSTABLE COMBUSTION IN SOLID ROCKET PROPELLANTS

L.A.Watermeier, W.P.Aungst and S.P.Pfaff

BRL Report No. 1168 July 1962

DA Proj No. 517-06-002, OMSC No. 5010.11.585

UNCLASSIFIED Report

UNCLASSIFIED

Rocket propellants - Combustion

Combustion - Photographic analysis


Composite - double base rocket propellant slabs which contained different concentrations and particle sizes of aluminum were burned in a transparent-walled chamber. The chamber was exhausted to the atmosphere. The slabs were ignited in cigarette fashion and burned under ambient nitrogen pressures of 200-800 psi. Experimental runs were made under steady flow conditions and under oscillating conditions with a siren rotating over the exhaust port.

Motion pictures were taken of the burning process at high framing rates. Data on droplet burning and concentrations in various regions above the propellant surfaces were obtained from individual frames of the film.

The rate of growth and rate of burning or evaporation of the aluminum droplets on the surface and in the flame zone are discussed. Agglomeration of aluminum on the propellant surface was appreciable and was a function of chamber pressure and initial aluminum concentration.



AD _____ Accession _____

Ballistic Research Laboratories, APG

AN EXPERIMENTAL INVESTIGATION OF POSSIBLE ALUMINUM ADDITIVE CONTRIBUTIONS TO UNSTABLE COMBUSTION IN SOLID ROCKET PROPELLANTS

L.A.Watermeier, W.P.Aungst and S.P.Pfaff

BRL Report No. 1168 July 1962

DA Proj No. 517-06-002, OMSC No 5010.11.585

UNCLASSIFIED Report

UNCLASSIFIED

Rocket propellants - Combustion

Combustion - Photographic analysis

Composite - double base rocket propellant slabs which contained different concentrations and particle sizes of aluminum were burned in a transparent-walled chamber. The chamber was exhausted to the atmosphere. The slabs were ignited in cigarette fashion and burned under ambient nitrogen pressures of 200-800 psi. Experimental runs were made under steady flow conditions and under oscillating conditions with a siren rotating over the exhaust port.

Motion pictures were taken of the burning process at high framing rates. Data on droplet burning and concentrations in various regions above the propellant surfaces were obtained from individual frames of the film.

The rate of growth and rate of burning or evaporation of the aluminum droplets on the surface and in the flame zone are discussed. Agglomeration of aluminum on the propellant surface was appreciable and was a function of chamber pressure and initial aluminum concentration.



AD _____ Accession _____

Ballistic Research Laboratories, APG

AN EXPERIMENTAL INVESTIGATION OF POSSIBLE ALUMINUM ADDITIVE CONTRIBUTIONS TO UNSTABLE COMBUSTION IN SOLID ROCKET PROPELLANTS

L.A.Watermeier, W.P.Aungst and Samuel P. Pfaff

BRL Report No. 1168 July 1962

DA Proj No. 517-06-002, OMSC No. 5010.11.585

UNCLASSIFIED Report

UNCLASSIFIED

Rocket propellants - Combustion

Combustion - Photographic analysis

Composite - double base rocket propellant slabs which contained different concertrations and particle sizes of aluminum were burned in a transparent-walled chamber. The chamber was exhausted to the atmosphere. The slabs were ignited in cigarette fashion and burned under ambient nitrogen pressures of 200-800 psi. Experimental runs were made under steady flow conditions and under oscillating conditions with a siren rotating over the exhaust port.

Motion pictures were taken of the burning process at high framing rates. Data on droplet burning and concentrations in various regions above the propellant surfaces were obtained from individual frames of the film.

The rate of growth and rate of burning or evaporation of the aluminum droplets on the surface and in the flame zone are discussed. Agglomeration of aluminum on the propellant surface was appreciable and was a function of chamber pressure and initial aluminum concentration.



AD _____ Accession _____

Ballistic Research Laboratories, APG

AN EXPERIMENTAL INVESTIGATION OF POSSIBLE ALUMINUM ADDITIVE CONTRIBUTIONS TO UNSTABLE COMBUSTION IN SOLID ROCKET PROPELLANTS

L.A.Watermeier, W.P.Aungst and Samuel P. Pfaff

BRL Report No. 1168 July 1962

DA Proj No. 517-06-002, OMSC No. 5010.11.585

UNCLASSIFIED Report

UNCLASSIFIED

Rocket propellants - Combustion

Combustion - Photographic analysis

Composite - double base rocket propellant slabs which contained different concentrations and particle sizes of aluminum were burned in a transparent-walled chamber. The chamber was exhausted to the atmosphere. The slabs were ignited in cigarette fashion and burned under ambient nitrogen pressures of 200-800 psi. Experimental runs were made under steady flow conditions and under oscillating conditions with a siren rotating over the exhaust port.

Motion pictures were taken of the burning process at high framing rates. Data on droplet burning and concentrations in various regions above the propellant surfaces were obtained from individual frames of the film.

The rate of growth and rate of burning or evaporation of the aluminum droplets on the surface and in the flame zone are discussed. Agglomeration of aluminum on the propellant surface was appreciable and was a function of chamber pressure and initial aluminum concentration.